M. Olivucci (Editor)
Computational Photochemistry
Theoretical and Computational Chemistry, Vol. 16

II. *Ab Initio* Methods for Excited States

Manuela Merchán and Luis Serrano-Andrés

Departamento de Química Física
Instituto de Ciencia Molecular
Universitat de València
Dr. Moliner 50, Burjassot
ES-46100 Valencia, Spain
Tel. 34 963543155/34 963544333
Fax. 34 963543156
Email: Manuela.Merchan@uv.es, Luis.Serrano@uv.es

1. INTRODUCTION

From the perspective of a chemist all sort of matter is essentially composed by a few types of elementary particles that can be combined in different ways. These particles do not follow the laws of classic mechanics but behave according to the laws of quantum mechanics. They present certain features, such as symmetry laws and exchange phenomena, without correspondence in a Newtonian world, which have to be taken into account theoretically. Constitution of matter is, therefore, a quantum-chemical problem involving many particles.

Knowledge on *ab initio* grounds of the true solutions for the full non-relativistic time-independent Schrödinger equation of molecules, within the Born-Oppenheimer approximation, has been considered as one of the Grand Challenge problems in science since the birth of quantum mechanics at the beginning of the twentieth century. The term "*ab initio*" is Latin and the English meaning is "from the start", that is, from the first principles, implying that no parametrization at all is employed. Unfortunately, the Schrödinger equation for a molecule, except for small systems, cannot be exactly solved at present and we are forced to look for appropriate algorithms to obtain approximate solutions. Within the framework of a particular technique (variation principle, perturbation theory, or other schemes), the procedure can be still performed at the *ab initio* level. With the need of methodological development, the discipline of Quantum Chemistry emerged and, in order to perform the applications of interest, a large number of approximate quantum-chemical methods is currently available. The main ideas for many of those methods come from the earliest methodological attempts but significant new algorithms have been developed and implemented into efficient software in the last decade.

Chemists have been some of the most active and innovative participants in the rapid expansion of computational science. Computational chemistry can be regarded as the

application of chemical, mathematical, and computing skills to the solutions of chemical problems. Obtaining approximate solutions to the Schrödinger equation is the basis for most of the computational chemistry performed today. The quantum-chemical applications performed serve many times as source of inspiration for new methodological developments. In what follows we shall consider reliable *ab initio* methods, those that offer reasonable answers for well-defined chemical problems. In practice, it is usually difficult to find a given method that can be applied to the successful calculation of many distinct chemical properties. Consequently, it is of major importance the selection of the proper method to be employed in the computation of a given molecular property. In the present chapter, we shall focus our attention mainly on the performance of *ab initio* methods for the description of spectroscopic molecular properties of compounds. The material presented is probably biased to our own work, but a fair coverage or other viewpoints can also be found.

2. GENERAL OVERVIEW

Most of the quantum-chemical methods developed up to date have been based on the concept of the one-electron wave function. The electronic states of a system with N electrons can be described by a double expansion. Molecular orbitals (MOs) are one-electron wave functions expressed as linear combinations of a known one-electron basis set {K} and the N-electron wave function is formulated in a many-electron basis set formed by determinants (or linear combination of them to form spin-adapted wave functions), built as normalized antisymmetric products of MOs. In principle, if the one-electron basis set {K} is complete, and a complete many-electron basis set can be generated by considering all possible occupations for the corresponding MOs, the true solution of the Schrödinger equation can be achieved. Such a computation is not possible technically in most cases and in actual applications the one-electron basis set has somehow to be truncated. Nevertheless, when *all* the N-electron wave functions are taken into account, the calculation is named *full configuration interaction* (FCI) and the corresponding eigenvalues and eigenvectors computed are exact within the space spanned by the finite basis set. Despite the great advances in FCI technology in the last few years, the size of the eigenvalue problem becomes rapidly too large to be handled by modern computers. As a result, FCI solutions are only available for relatively small molecular systems. We have, unfortunately, to land in the field of truncations, in both the one- and many-electron basis sets. Truncations performed in the one-electron basis sets together with the limitations introduced in the many-electron basis sets, which are normally truncated at a given degree of excitation (considering up to singly, doubly, triply, ... excited determinants) are the most important source of inaccuracies in the quantum-chemical calculations. The type of truncations carried out in conjunction with the class of techniques employed (variation principle, perturbation theory, and others) characterizes most of the methods currently employed through the available commercial software.

Since the ground state of a large number of molecules at the equilibrium geometry is well described qualitatively by a single electronic configuration, it is not surprising that great

efforts have been devoted in the development of treatments such as Møller-Plesset perturbation theory (MP2, MP3, MP4), singles and doubles configuration interaction (CISD), and related non-variational approaches like coupled-electron pair approximation (CEPA), as well as coupled-cluster (CC) methods, in which the starting point is the Hartree-Fock (HF) wave function [1–4]. In contrast, the situation is quite different for the description of electronically excited states, which normally have several configurations equally relevant. The same may occur in certain regions of the ground-state hypersurface, far away from the equilibrium structure, for instance, in a transition state (TS) or in the dissociation limit of a homolitic breaking process of a covalent bond. In order to gather satisfactory results, one has to supply a wave function bearing enough flexibility to treat the required number of configurations on an equal footing. The goal can be nicely accomplished by the multiconfigurational self-consistent field (MCSCF) approach. For just a single configuration, it is equivalent to the MO model most commonly used in quantum chemistry: the HF SCF procedure. The complete active space SCF (CASSCF) is a variant of the MCSCF method that has become particularly popular because of its technical and conceptual simplicity. In the CASSCF method the active electrons are distributed among the active orbitals in all possible ways consistent with a given spatial and spin symmetry of the electronic state. The number and nature of the active orbitals and electrons are decided by the user. Normally, it is a crucial step for the successful performance of the approach, which must be guided by a deep knowledge of the chemical process under consideration in order to offer the required flexibility. It is not a question of chemical intuition but of chemical knowledge. Nothing easier than getting meaningless CASSCF results if the active space is meaningless for a given application. It is worth mentioning at this point that the ultimate responsibility for the selection and use of a given method relies on the user. For this purpose, calibration calculations are often enlightening. At the CASSCF level one usually takes into account long-range effects related to the so-called non-dynamic (static) correlation effects, making it possible the proper treatment of several nearly degenerate configurations. The remaining electron correlation effects, associated with the instantaneous short-range electron-electron interaction, can be accomplished by using variational methods like muti-reference CI (MRCI) [5–9] or employing perturbation theory by means, for instance, of the CASPT2 method (complete active space perturbation theory to second order) [10–12] or other related multireference perturbation theory (MRPT) schemes [13, 14].

According to the number of configurations considered initially, the methods can be classified in the following two categories:

- Single-configuration methods. They are typically based in the HF reference, which determines the MOs. The electron correlation treatment is usually performed at the CI, CC or MP levels. The coupled-cluster methods with singly and doubly configurations including the effect of triple excitations by perturbation theory CCSD(T), as well as related approaches, may yield accurate results. In general, the applicability of the methods in this group is restricted to situations where a single reference wave function is adequate for the description of a chemical process.

- Multiconfigurational methods. Part of the electronic correlation is already included in the reference wave function, normally by using a MCSCF wave function, which determines a set of MOs. The remaining electron correlation effects are accounted for by MRCI, MRCC or MRPT techniques. They have a more ample range of applicability (ground state, excited states, TS, ...).

The accurate CASSCF/MRCI protocol is computationally demanding, and quite often is not tractable, because a satisfactory selection of the active space requires huge technical resources. On the other hand, since a decade ago the multiconfigurational second-order perturbation theory CASPT2 has shown to be an efficient alternative, yielding an advantageous rate between the quality and the computational cost for the description of excited states in systems of relatively large molecular size [15–18]. Apart from MRCI, CASPT2 and other different MRPT algorithms, a quick inspection of the recent literature on excited states reveals that the following methods are also used quite often: CI-singles (CIS) [19], Random-Phase Approximation (RPA) and related approaches [20], as well as coupled-cluster based methods, Symmetry-Adapted Cluster CI (SAC-CI) [21], Equation-of-Motion CC (EOM-CC) [22], and linear response CCn [23]. They shall be reviewed in Section 4 from a practical point of view, making special emphasis on the expected advantages, disadvantages, and applicability in the qualitative/quantitative understanding of the electronic states. In addition, the performance of the time-dependent density functional (TD-DFT) approach, which is becoming widely used for the treatment of excited states, shall also be discussed. Because of the primordial role that electronic correlation plays in the relative placement of electronic states, the essentials shall be considered separately in the next section.

3. ELECTRON CORRELATION IN MOLECULES

The extended treatment of electron correlation has traditionally been the bottleneck to achieve accurate results for excited states. Therefore, let us consider in this section the meaning of electron correlation in molecules from different perspectives.

The major goal in quantum-chemical methodology for a molecular system formed by N electrons (i, j, ..) and M nuclei (A, B, ..) is finding reliable approximate solutions of the stationary electronic states as solutions of the Schrödinger equation

$$\hat{H}\,\Phi = \varepsilon\,\Phi \qquad (1)$$

where the electronic wave function Φ depends explicitly on the N electronic coordinates $\mathbf{x}_1$, $\mathbf{x}_2$, $\mathbf{x}_3$,...$\mathbf{x}_N$ and parametrically on the nuclear coordinates, within the well-known Born-Oppenheimer approximation. The three spatial coordinates $\mathbf{r}_i$ and the one spin coordinate ω_i are denoted collectively by $\mathbf{x}_i$. In atomic units (au), the electronic Hamiltonian operator is

$$\hat{H} = -\frac{1}{2}\sum_{i=1}^{N}\nabla_i^2 - \sum_{i=1}^{N}\sum_{A=1}^{M}\frac{Z_A}{r_{iA}} + \sum_{i=1}^{N}\sum_{j>i}^{N}\frac{1}{r_{ij}} \qquad (2)$$

The first term in Eq. (2) describes the kinetic energy of the electrons; the second term represents the Coulomb attraction between electrons and nuclei; the third term corresponds to the repulsion between electrons. The total energy for fixed nuclei includes the nuclear repulsion, a constant at a given geometry,

$$\varepsilon_{tot} = \varepsilon + \sum_{A=1}^{M} \sum_{B>A}^{M} \frac{Z_A Z_B}{R_{AB}} \tag{3}$$

and provides a potential for the nuclear motion. Eq. (1) constitutes the electronic problem, which has been during decades of major concern in methodological developments.

The physics of electron correlation is hidden in the Hamiltonian itself. The Coulomb repulsion given by the term r_{ij}^{-1}, the inverse distance between two electrons, increases enormously in the regions close to $r_{ij} = 0$, preventing that two electrons may occupy the same space. Therefore, the motion of any two electrons is not independent but it is correlated. The phenomenon is known as *electron correlation*. Moreover, the statement that two electrons are correlated is equivalent to express that the probability of finding two electrons at the same point in space is zero. The instantaneous position of electron *i* forms the centre of a region that electron *j* will avoid. For this reason, it is stated that each electron, as described by the exact wave function Φ, is surrounded by a *Coulomb hole*. However, electron correlation is not taken into account properly by many approximate methods. The effect of neglecting electron correlation partly in approximate quantum-chemical approaches has great impact in the molecular spectroscopic properties of interest (computed transition energy, nature of the electronically excited states, related oscillator strengths, etc).

The simplest wave function to describe a many-electron system is a Slater determinant built by orthogonal one-electron wave functions. Electrons are fermions and accordingly they have to be described by an antisymmetric wave function. For an N-electron system the Slater determinant has the form

$$\Psi = \frac{1}{\sqrt{N!}} \begin{vmatrix} \chi_1(\mathbf{x}_1) & \chi_2(\mathbf{x}_1) & \cdots & \chi_N(\mathbf{x}_1) \\ \chi_1(\mathbf{x}_2) & \chi_2(\mathbf{x}_2) & \cdots & \chi_N(\mathbf{x}_2) \\ \vdots & \vdots & & \vdots \\ \chi_1(\mathbf{x}_N) & \chi_2(\mathbf{x}_N) & \cdots & \chi_N(\mathbf{x}_N) \end{vmatrix} \tag{4}$$

The constant $(N!)^{-1/2}$ is a normalization factor. The wave function for an electron that describes both the spatial distribution and its spin is called spin orbital, $\chi_i(\mathbf{x}_i)$. Since the Hamiltonian employed does not depend on the electronic spin (see Eq. (2)), each spin orbital can be expressed by multiplying the spatial orbital, $\psi_j(\mathbf{r}_i)$, by the spin function, $\eta(\omega_i)$

$$\chi_i(\mathbf{x}_i) = \psi_j(\mathbf{r}_i)\, \eta(\omega_i) \tag{5}$$

A complete set for describing the spin of an electron consists of two orthogonal functions $\alpha(\omega_i)$ and $\beta(\omega_i)$. It accounts for the fact that to completely describe an electron is necessary to specify its spin. Therefore, within the non-relativistic framework, inclusion of the electronic spin is phenomenological. To simplify the notation, a normalized Slater determinant is represented by only showing the diagonal elements of the determinant, including the normalization factor

$$\Psi = |\chi_i(x_1)\,\chi_2(x_2)\cdots\chi_N(x_N)\rangle = |\chi_1\,\chi_2\cdots\chi_N\rangle \tag{6}$$

A single-determinant wave function has several interesting properties. Firstly, it is worth noting that spin orbitals must be linearly independent, otherwise the value of the determinant is zero. It is obvious that interchanging two rows of the Slater determinant, which is equivalent to interchanging the coordinates of two electrons, changes the sign of the determinant. The requirement of the antisymmetry principle is automatically fulfilled. Having two columns of the determinant identical, that is, two electrons occupying the same spin orbital, makes the determinant zero. Thus, no more than one electron can occupy a spin orbital (Pauli exclusion principle). When a linear transformation of the set $\{\chi_i\}$ is carried out,

$$\chi_i' = \sum_j^N \chi_j\, A_{ji} \tag{7}$$

where A_{ji} is an element of the matrix **A** of dimension NxN, with a value for its determinant, det(**A**), different from zero, then

$$\Psi' = \det(\mathbf{A})\,\Psi \tag{8}$$

The wave functions Ψ' and Ψ differ just in a constant and, therefore, represent the same physical situation. Since the set of spin orbitals is linearly independent, we can always choose a transformation matrix **A** so that the resulting spin orbitals χ_i' become orthonormal. Therefore, no restriction at all is imposed when we choose from the beginning an orthonormal set of spin orbitals. It just makes the computation of the Hamiltonian matrix elements involving Slater determinants easier. A Slater determinant is completely specified by the spin orbitals used to build it and any unitary transformation of them is equally valid. Two sets of spin orbitals related by a unitary transformation ($\mathbf{A}^\dagger = \mathbf{A}^{-1}$), which keeps the orthonormality of the spin orbitals, yield the same Slater determinant (see Eq. (8)). Slater determinants formed from orthonormal spin orbitals are normalized and N-electron Slater determinants that have different spin orbitals are orthogonal.

The Slater determinant fulfils the basic symmetry law derived from the identity principle, because it describes N electrons occupying N spin orbitals ($\chi_1\,\chi_2\cdots\chi_N$) without specifying which electron is in each orbital. From a physical viewpoint, the use of a Slater determinant

wave function to describe a many-electron system implies that we are immersed in a model of independent electrons, where the electrons are not correlated, and the Coulomb hole is discarded. Nevertheless, it can be easily demonstrated that in a Slater determinant the motion of two electrons with the same spin function is correlated, that is, the probability of finding two electrons with parallel spins at the same point in the space is zero, the so-called exchange correlation, which is incorporated by the antisymmetric condition of the wave function for fermions. The phenomenon is known as the Fermi hole. We are, therefore, facing a model of independent particles where the behavior of certain electrons is not fully independent, because the Fermi hole simulates somehow the Coulomb hole. Since the motion of electrons with different spin function remains uncorrelated (there is a finite probability of finding two electrons with opposite spins at the same point in space), a single determinant wave function is commonly referred as an uncorrelated wave function.

The Hartree-Fock approximation usually constitutes the first step towards more accurate approximations and has played a crucial role in elucidating modern chemistry. Indeed, many of the quantum-chemical methods can be considered either as simplifications of the HF method or going beyond it. The HF method provides the mathematical tools to obtain the unknown spin orbitals to build the best Slater determinant by making use of the variation principle. Let us consider a single Slater determinant to describe the ground state of an N-electron system

$$\Psi_0 = \left|\chi_1\chi_2\cdots\chi_a\chi_b\cdots\chi_N\right\rangle \tag{9}$$

The variation principle states that the *best* wave function of this functional form (single determinant type) is the one giving the lowest energy

$$E_0 = \left\langle\Psi_0\left|\hat{H}\right|\Psi_0\right\rangle \tag{10}$$

where $\hat{H}$ is the electronic Hamiltonian. By minimizing E_0 with respect to the choice of spin orbitals one can arrive to the Hartree-Fock conditions, which can be expressed in many different manners, and in particular the canonical expression takes the form

$$\hat{f}\chi_a = \varepsilon_a\chi_a \qquad a = 1...N \tag{11}$$

where $\hat{f}$ is an effective one-electron operator, called the Fock operator, which actually depends on its eigenfunctions. Thus, the HF equation (11) is not linear and must be solved iteratively through the SCF method. The Fock operator is the sum of a core-Hamiltonian operator and an effective one-electron potential operator. The former is the kinetic energy and potential energy for attraction to the nuclei and the latter is the average potential experienced by the electron described by the occupied spin orbital χ_a due to the presence of the remaining N-1 electrons. The solution of the HF eigenvalue problem, Eq. (11), yields a set of orthonormal canonical spin orbitals $\{\chi_m\}$ with orbital energies $\{\varepsilon_m\}$. The N spin orbitals with

the lowest energies are called occupied orbitals and span the Fock space. The remaining MOs, the virtual orbitals, span the complementary Fock space. Any unitary transformation within the Fock subspace leaves the HF energy invariant, Eq. (10). Transformations among the virtual orbitals can also be performed as long as the subspace spanned by the virtual spin orbitals remains orthogonal to the Fock subspace. They are particularly useful to improve (localize) the virtual MOs prior a MRCI calculation, which makes the convergence of the CI expansion more efficient [24].

In practice, the HF equation is solved by introducing a finite basis set of spatial basis functions $\{\phi_\mu \mid \mu = 1,2,...K\}$ resulting in different matrix equations: Roothaan equations for closed-shell restricted determinants, Pople-Nesbet equations for unrestricted determinants, and Roothaan-Hartree-Fock equations for open-shell restricted determinants [1, 25–27]. Increasing the flexibility of the one-electron basis set $\{\phi_\mu\}$, the HF energy E_0 will progressively reach a limit, called the Hartree-Fock limit (the exact HF energy). This limit cannot be usually achieved and the computed HF energy with a finite basis set is somewhat above it.

The correlation energy (E_{corr}) is defined as the difference between the exact non-relativistic energy of the system (ε_0) and the HF energy E_0 in the limit that the basis set approaches completeness

$$E_{corr} = \varepsilon_0 - E_0 \tag{12}$$

Since ε_0 is lower than E_0, the correlation energy is negative. Because of the use of a complete basis set is prohibitive, or simply impossible, the exact electron correlation of a system cannot be computed, except for small systems. Definition of E_{corr} corresponds then to the difference between the energy computed at a given level of the electron correlation treatment and the corresponding HF energy, both computed with the same, flexible enough, one-electron basis set $\{\phi_\mu\}$.

The HF wave function, as it is a Slater determinant, the best one indeed in the sense of the variation principle, enjoys the basic features discussed above for determinants. Therefore, the HF wave function is uncorrelated, which leads to certain limitations in actual applications. For instance, it is well known that the restricted HF method cannot describe the dissociation of molecules into open-shell fragments (*e.g.* $H_2 \rightarrow 2H$). Let us address this aspect with a model: the hydrogen molecule described in a minimal basis set, which also serves to introduce in a natural way more complicated functions including electron correlation.

In a minimal basis model of the H_2 molecule there are only two MOs, which are linear combinations of the two functions φ_A and φ_B placed on the nuclei H_A and H_B, respectively. The occupied molecular orbital, the bonding orbital of σ_g symmetry, has the lowest energy, and the virtual orbital corresponds to the antibonding combination of σ_u symmetry

$$\psi_2(i) = \frac{1}{\sqrt{2(1-s)}}\left(\varphi_A(i) - \varphi_B(i)\right) \qquad ---- \qquad (\sigma_u^*) \qquad (13)$$

$$\psi_1(i) = \frac{1}{\sqrt{2(1+s)}}\left(\varphi_A(i) + \varphi_B(i)\right) \qquad --\uparrow\downarrow-- \qquad (\sigma_g)^2 \qquad (14)$$

where $s = \langle \varphi_A | \varphi_B \rangle$ is the overlap between the basis functions. The case is simple enough that the solutions to Roothaan's equations are determined by symmetry arguments. The symmetry of the breaking process is maintained along the dissociation path and, therefore, the MOs have the same form independently of the interatomic distance R. Close to the equilibrium geometry, the ground-state wave function is

$$\Psi_0\left({}^1\Sigma_g^+, R = R_{opt}\right) = \left|\psi_1\,\overline{\psi}_1\right\rangle \qquad (15)$$

which expanded in terms of the basis functions leads to

$$\Psi_0\left({}^1\Sigma_g^+, R = R_{opt}\right) = \frac{1}{2(1+s)}\left(\left|\varphi_A\overline{\varphi}_A\right\rangle + \left|\varphi_B\overline{\varphi}_B\right\rangle + \left|\varphi_A\overline{\varphi}_B\right\rangle + \left|\varphi_B\overline{\varphi}_A\right\rangle\right) \qquad (16)$$

In Eq. (16), the first and second terms correspond to ionic configurations in the valence bond (VB) theory $H_A^-\ H_B^+$ and $H_A^+\ H_B^-$, respectively, while the third and fourth terms represent covalent situations. The four terms share the same coefficient, therefore, their weight is the same at a given distance R. Consequently, as $R \to \infty$, $s \to 0$, and the dissociation limit obtained is

$$E_0 = \frac{\left\langle \Psi_0 \left| \hat{H} \right| \Psi_0 \right\rangle}{\left\langle \Psi_0 | \Psi_0 \right\rangle} = \frac{1}{4}\left(4\,E(H) + 2\,E(H^-)\right) = E(H) + \frac{1}{2}E(H^-) \qquad (17)$$

The limit, rather than being twice the energy of the hydrogen atom in the same basis set (2E(H)), includes the spurious term $E(H^-)/2$ reflecting the contribution of the ionic structures even at infinity. However, the incorrect behavior of the restricted HF theory at long interatomic distances for systems that dissociate into open-shell products does not detract from the validity of the approach around the equilibrium geometry, where the HF method has been shown to be remarkably successful for closed-shell ground-state systems.

The ground state of the H_2 system in the dissociation limit corresponds to two ground-state hydrogen atoms (^2S) and the correct spin adapted wave function is

$$\Psi_0\left({}^1\Sigma_g^+, R = \infty\right) = \frac{1}{\sqrt{2}}\left(\left|\varphi_A\overline{\varphi}_B\right\rangle - \left|\overline{\varphi}_A\varphi_B\right\rangle\right) \qquad (18)$$

that in terms of MOs (Eqs. (13) and (14) with s = 0) can be rewritten as

$$\Psi_0\left({}^1\Sigma_g^+, R=\infty\right)=\frac{1}{\sqrt{2}}\left(\left|\psi_1\overline{\psi}_1\right\rangle-\left|\psi_2\overline{\psi}_2\right\rangle\right) \tag{19}$$

The previous expression suggests that in order to decrease the weight of ionic determinants in Eq. (16) at interatomic distances close to the equilibrium geometry, $R=R_{opt}$, one has to combine the determinants corresponding to the ground-state $(\sigma_g)^2$ and doubly excited $(\sigma_u^*)^2$ configurations. The procedure is known as the configuration interaction (CI) method

$$\Psi_{CI}=\left|\psi_1\overline{\psi}_1\right\rangle+\lambda\left|\psi_2\overline{\psi}_2\right\rangle \tag{20}$$

being $\lambda< 0$ the variational parameter. As $R\rightarrow\infty$, then $\lambda \rightarrow -1$, and the functions (20) and (19), except for a normalization factor, become equivalent. The method offers a proper treatment of the spatial correlation of the electrons, called left-right correlation, making it possible that the two electrons belong to different nuclei. In summary, in order to get a correct dissociation the doubly excited configuration involving the antibonding orbital has to be invoked because it has at infinity the same weight as the closed-shell ground-state configuration.

Alternatively, one could think that the unrestricted HF (UHF) approximation might be a solution. It can be shown that the UHF energy goes to the correct limit but the total wave function does not. The UHF solution for the H_2 molecule is not a pure singlet but it is contaminated by a triplet, which is required to make the UHF wave function a single determinant. At the dissociation limit the triplet contamination represents 50% of the wave function. Therefore, an unrestricted solution does not provide the best starting point neither for configuration interaction nor perturbation calculations.

A similar reasoning employing CI wave functions can be also performed to analyze the two-electron correlation relative to the nuclear positions. These short-range correlation effects are typically called radial and angular correlation. They are related to the larger preference, in relation to the HF description, that two electrons actually have to be far apart of each other: close/far from the nucleus of an atom (radial) and in opposite ways in a given direction, up/down, in the space surrounding the nucleus (angular). It is worth noting, however, that approaches based on many-electron basis sets (determinants or Configuration State Functions, CSFs) built as products of one-electron wave functions (orbitals) cannot represent exactly the shape of the Coulomb hole, although it becomes reasonably described with large CI expansions. Unfortunately, as stated above, the convergence of the CI expansion is slow. The reader is referred to the interesting and recent contribution reported by Knowles, Schütz, and Werner for a more detailed discussion on the topic [14].

In molecular systems, electron correlation is usually computed in two steps. Firstly, non-dynamic electron correlation is accounted for by using a CASSCF wave function or a selected

number of configurations. In a second step, the remaining electron correlation effects (dynamic correlation) are estimated by considering the singly and doubly replacements from the MRCI or the CASSCF wave functions. The borderline between non-dynamic (static) and dynamic correlation is not clearly defined in most cases. Normally, correlation energy arising from long-range terms allowing the correct asymptotic behavior in a molecular dissociation is referred to as non-dynamic correlation. The remaining correlation energy dealing with short-range effects relevant in describing the Coulomb hole as accurate as possible is associated with dynamic correlation. Inclusion of both types of correlation is crucial in order to gather accurate results. For instance, a good (uncorrelated) HF SCF calculation tends to underestimated bond lengths with respect to a (reliable, gas phase) datum determined experimentally because in a HF wave function the ionic and covalent terms (in the VB sense) are equally weighted, making single covalent bonds too tightly bound. As can be easily deduced from Eq. (20), non-dynamic electron correlation decreases the effect of ionic forms in the CI wave function, leading to too long bond distances. A subsequent introduction of dynamic correlation recovers such an overestimation, leading the computed geometry to a closer agreement with the experimental datum.

One of the most efficient manners of dealing with non-dynamic electron correlation is by using the CASSCF wave function comprising as active the valence MOs and valence electrons. For instance, it leads in a diatomic molecular system to the correct dissociation limit, that is, to the sum of the energies for the isolated atoms. This property is termed size-consistency, which requires that the energy of two non-interacting systems be the sum of the individual system energies. Many of the contributions of the valence CASSCF are not actually required to get the adequate dissociation limit. Shorter MCSCF wave functions would equally make it correctly, as the GVB-PP approach, which becomes equivalent to a selected pair-wise MCSCF wave function, but the valence CASSCF is still preferred because its implementations have technical advantages that, in general, make the computation easier. However, the idea that the valence CASSCF wave function is the most general way to obtain a proper treatment of non-dynamic electron correlation leads sometimes to surprises. For instance, the valence CASSCF yields for the water molecule to an asymmetric structure, with two non-equivalent O-H bonds. The right C_{2v} structure can be recovered by enlarging the active space with an extra orbital which makes then the calculation balanced with respect to the treatment of both bonds (see discussion in Ref. [28]). Thus, the idea that the best choice of active orbitals corresponds to the valence MOs is not always supported, although the fact that valence electron correlation is linked to non-dynamic correlation effects holds true.

In the computation of excited states for small-medium molecular systems, the valence excited states are usually interleaved among a number of Rydberg states. Therefore, the one-electron basis set has to be flexible enough to compute both valence and Rydberg states. Consequently, the active space has to include the necessary valence and Rydberg MOs. In those situations, the CASSCF wave function takes into account some dynamic and non-dynamic electron correlation. In summary, selection of the active space has to be performed in accordance with the application at hand. It is not a black-box procedure and might not be

straightforward, although is far from being impossible because there is a large body of information accumulated. As in any scientific research, one has to become familiar with the available literature on the issue prior the actual computation gets started. In this sense, the choice of the active space for CASSCF calculations is not an exception. The effort is rewarding because, when a proper CASSCF wave function is employed as reference function for a subsequent treatment of dynamic correlation (MRCI or MRPT), the results are accurate within 0.1-0.2 eV, which is an error bar sufficient for many spectroscopic applications. Otherwise, if higher accuracy were required the whole selection procedure for the proper methodology has to be redone. For instance, in the description of weak interacting systems like in the NO dimer, N_2O_2 [29], the Averaged Coupled-Pair Functional (ACPF) [30] method was preferred because it is strictly size-extensive, that means it has the correct scaling with the number of particles, whereas any other forms of truncated CIs, as well as the CASPT2 method, are not [14, 16].

The natural orbitals (NOs) derived from a Restricted Active Space SCF (RASSCF) calculation, an extension of the CASSCF method [31], are a good choice for a single-root MRCI computation [32]. Natural orbitals are defined as density matrix eigenvectors. Since the trace of the density matrix is equal to the number of electrons, the associated eigenvalues are interpreted as the corresponding occupation numbers of the NO. It can be shown that for two-electron systems, a CI wave function written in terms of doubly excited determinants built from NOs offer the most compact one-electron basis set [1, 14]. Implicit to a variational calculation is the fact that the largest contributions come from pairs of electrons occupying the same region of physical space ($\sigma_1, \sigma_1^*; \pi_1, \pi_1^*$; etc). One of the best manners of localizing a pair of MOs in a given spatial region is through a pair-wise MCSCF computation; the decrease of the energy associated with that pair of electrons to fulfill the variation principle is directly related to the increase of the corresponding exchange integral between the two MOs. As larger is the exchange integral involving a pair, more localized the two MOs would become. The main effect is carried out on the virtual MO of the pair, especially when canonical MOs are used as starting point. Virtual canonical MOs are computed in the mean field of N electrons, and therefore they become too diffuse. In contrast, the occupied canonical MOs are properly obtained in the mean field of the remaining N-1 electrons. In general, canonical MOs represent the most inefficient choice of one-electron basis set for the purpose of CI calculations. The convergence of the CI expansion is significantly improved with a set of localized MOs. Among many different choices of MOs available, the best corresponds to NOs derived from an MCSCF calculation [24]. The CASSCF/MRCI approach is capable of yielding accurate results on medium size molecules as shown in the eighties by many authors, in particular Bauschlicher and co-workers [33].

4. *AB INITIO* METHODS: ESSENTIALS FOR EXCITED STATES

In order to write the present section, two criteria have been used. Firstly, the methods included respond to the fact they are frequently used for the study of excited states, as it can

be easily checked from a rapid search on papers published during the last few years. However, it does not mean that in the authors' opinion all of them are appropriate for the treatment of excited states. It just reflects in certain cases that, despite of their well-known limitations, they are commonly used nowadays. Secondly, in an attempt to keep this contribution as practical as possible for a researcher interested in using *ab initio* methods for computational chemistry, the methodological details are kept to the minimum. In order to get further insight into the methods, the reader is referred to the original papers or more advanced material. Advantages and disadvantages on the applicability of the corresponding approaches shall, however, be emphasized. According to the classification introduced in Section 2, under the headings single-configuration and multiconfigurational methods, as appropriate, the most popular approaches used today are next discussed.

4.1. Single-configuration methods

Within the molecular-orbital model, the simplest manner to describe the excited states of a molecule that one can think of is by one- (or two)-electron promotion(s) from the occupied to the virtual canonical MOs obtained from the SCF calculation at the equilibrium geometry of the corresponding ground state. Within this scheme, the energy difference of two orbital energies can be related to the vertical excitation energy absorbed by a molecular system. The smallest energy difference occurs between the lowest unoccupied molecular orbital (LUMO) and the highest occupied molecular orbital (HOMO). That the excited state described mainly by the HOMO→LUMO one-electron promotion does not always correspond to the lowest-energy transition is strongly supported by high-level *ab initio* results, as well as experimental evidence [15–18]. In summary, this simple approach usually yields predictions that might not be even correct qualitatively. Nevertheless, analysis of the leading configurations of a complicated multiconfigurational wave function on the basis of the corresponding NOs, which are topologically similar to the canonical MOs, is very helpful. In fact, this is the underlying meaning of an excited state labeled, for instance, as HOMO→LUMO coming from an extended CASSCF computation.

Giving a step forward, a vertical excitation energy can be estimated by two HF/UHF SCF calculations of the respective ground and excited states. As it occurs also in the computation of ionization potentials at the HF level, the accuracy of the result for the lowest excited state, independently of its multiplicity, strongly depends on the molecule under consideration. The source of the errors is related to the intrinsic limitations of the HF approach: lack of electron correlation and spin contamination for an unrestricted open-shell wave function. Because only exchange correlation is included, UHF triplet states are strongly favored with respect to open-shell singlet states, which leads to the wrong ground state for some biradicals [34]. All these approaches are sometimes known as the ΔSCF method [2, 35].

The next step in complexity leads to the widespread method called CIS (Configuration Interaction-Singles) [19]. The essence of the method is to consider that an excited state can be described by a singly excited determinant formed by replacing, with respect to the HF wave function, an occupied spin orbital with a virtual spin orbital. The drawbacks of such a

description may be partially compensated if a linear combination of all possible single excited determinants (φ_i^a) is used to build the excited state wave function as:

$$\Psi_{CIS} = \sum_{i}^{M}\sum_{a}^{N} c_{iak}\varphi_i^a \qquad (21)$$

where the coefficients c_{iak} are the components of the eigenvector for state k, M is the number of occupied orbitals (i) from which excitation is allowed, and N the number of virtual orbitals (a) into which excitation is considered. The singly excited states are orthogonal to the ground state because of the Brillouin theorem, but not necessarily to each other. The orthogonalization of the states is the essence of the CIS (CI-Singles) technique. The CI-singles procedure involves diagonalization of the CI matrix formed from the HF reference and all single excited configurations. The final outcome is a set of energy eigenvalues associated with eigenvectors in which the coefficients of the singly excited determinants, variationally obtained, characterize the state. The technique is size-consistent, allows spin flips in the excited electrons, and therefore to describe singlet and triplet wave functions, and also to obtain analytical gradients [19]. The description of the ground state in the CIS method is kept at the HF level. The CIS method clearly differs from a ground-state CI calculation in the sense that the former simply requires from the ground state the optimal HF MOs and the CI is performed to orthogonalize the singly excited states, while the latter includes CI excitations, higher than singles, to improve the description of the ground state itself.

The main flaw of the CIS method is the lack of correlation energy. Further attempts to solve the problem by using double excitations [36] or perturbation theory [19] were not successful. Improved results have been obtained with semiempirical parametrizations of the CIS matrix elements, for instance using the INDO/S approach [2]. In general the CIS excitation energies are largely overestimated due to the absence of electron correlation energy. For instance, a calculation on the singlet excited states of benzene reported a mean absolute error of 0.7 eV, with deviations as large as 1.4 eV, although larger errors are common [37]. Despite the claims that the results are qualitatively useful because the states are correctly ordered [2], the facts speak to the contrary. There are more cases in the literature [38-40] of failures in the prediction of the CIS energy ordering that successes, simply because the differential correlation energy affects the excited states unevenly and because the intrinsic character of the states is multiconfigurational. The well-known 2^1A_g state of polyenes, one of the main protagonists of their photochemistry, is a good example. For *trans*-1,3-butadiene there is no CIS ^1A_g $\pi\pi^*$ valence excited state below 9.0 eV [41], more than 3 eV higher than most of high-quality multiconfigurational methods [42, 43]. In a CASSCF description, the doubly excited configurations contribute by 42% to the state wave function. CIS, as most of the single-configuration methods, will have enormous problems to describe such states. In systems were purely doubly excited states exist at low energies [44], these methods cannot even represent such states. In summary, the CIS method is clearly unsafe and its use is discouraged because the obtained results are usually misleading [38–40].

A large number of methods to compute excited states is included under the denomination of propagator approaches [20]. As such, the underlying technique, also called Green's function approach, equation-of-motion or linear response theory in its different formulations, can be applied to various types of methodologies whether single- or multiconfigurational configuration interaction, coupled-cluster, or density functional. The basis of the technique considers that once a molecule is subjected to a linear time-dependent electric field fluctuating with frequency ω, a second-order property as the frequency-dependent ground-state polarizability of the system is well approximated by

$$\alpha_{\omega} = \sum_{i \neq 0}^{states} \frac{\left| \langle \Psi_0 | r | \Psi_i \rangle \right|^2}{\omega - \Delta E_i} \qquad (22)$$

where the denominator of the expression involves the frequency of the field and the excitation energies (ΔE_i) characterizing the excited states (i), while the numerator of each term is the square of the transition dipole moment between the ground and the corresponding excited state [2, 20]. Using complex function analysis it is possible to obtain the poles of the expression, that is, the values for which the frequency corresponds to the excitation energies and the denominator goes to zero, while the residues provide the numerators, in this case the one-photon absorption matrix elements. Higher-order quadratic response theory determines third-order molecular properties, as the first hyperpolarizabilities, and from them two-photon absorption matrix elements [45]. The peculiarity of the propagator approaches is that the wave functions of the individual states are not necessarily computed to obtain excitation energies and transition probabilities, while its quality relies on the type of reference wave function.

A hierarchy of approximate propagator methods can be defined as function of the selection of the order of the particle-hole replacement operators. The most popular among the polarization propagator methods is the Random-Phase Approximation (RPA) or Time-Dependent Hartree-Fock (TDHF) approach, where the used reference is the HF ground state and a single replacement operator is employed [20], and that is equivalent to the Coupled Hartree-Fock (CHF) approximation for time-independent perturbing fields [46]. Further developments of the method have included second-order perturbation (MP2) based approaches such as the Second-Order Polarization Propagator Approach (SOPPA) method, in which the so-called density-shift terms, particle-particle and hole-hole, are included [47, 48]. Many other variants have been developed, but our goal is not to perform a systematic review [20]. Just to mention the second- and third-order Algebraic-Diagrammatic Construction (ADC) approach, a Green's function one-electron propagator approach which has been applied in recent years to several problems [49]. Methods based on Green's function belong to the same hierarchy of approaches. They are typically expressed in the energy-dependent formalism, which can be transformed to the time-dependent propagator formalism by using a Fourier transform. One-particle many-body Green's functions methods are basically employed to compute ionization potentials (IPs) and electron affinities (EAs) [1].

Usual errors of the RPA method fall into ±1-2 eV in the excitation energies, while oscillator strengths may differ in one order of magnitude. It is also frequent to find singlet and triplet instabilities [47]. The effect of double excitations has been included by perturbation theory in order to slightly improve the excitation energies in the RPA(D) approach [50]. The SOPPA approach may improve the results within ±0.6 eV. A similar behavior is displayed by the ADC(2) method, slightly improved in the third-order version [49]. In any case, all these methods do not include non-dynamic correlation effects and, because of their single-configuration character, are extremely deficient when computing multiconfigurational states. Moreover, they cannot treat double excited states or open-shell ground-state excited states [47]. As a general advice, the improved versions of the methods, SOPPA and ADC(3), can be used to obtain a good qualitative description of the spectrum, although they lack generality. Compared to other methods they have, supposedly, the desired black-box behavior, and with respect to the TD-DFT approaches, their failures are not erratic, but well justified. Multiconfigurational response methods have been developed in recent years proving to be accurate in the calculation of molecular properties, not so much on energies [51], because of the lack of dynamical correlation.

The most recent family of methods for excited states based on a single reference that have known practical use, at least for small systems, are those based on the size-extensive coupled-cluster (CC) approach. CC methods for the ground state have become, in practice, the most accurate quantum-chemical approaches for many systems. Exceptions are however well recognized, which are related to low levels of excitations employed in situations where the single-configuration reference is clearly poor, for instance dissociating or quasi-degenerated situations or systems like ozone, C_2, N_2, the NO dimer and others [2, 35, 52–54]. The key point of single-configuration CC approaches for excited states is that they use a HF zeroth-order reference, which is in general rather poor to represent excited states, and, in order to recover a large amount of correlation, high orders in the excitation level have to be included [55].

Three groups of methods have been most employed: the Symmetry-Adapted Cluster Configuration Interaction (SAC-CI) approach [21], the Equation-of-motion Coupled-Cluster (EOM-CC) method [22], and the hierarchy of linear response CCn approaches [23]. Although they have different formulations, their performance for the common truncated and non-approximated coupled-cluster models is similar. The SAC-CI method, which has been used to compute very large systems by approximate procedures [56], and has been also extended to open-shell references [57], is comparable to the EOM-CCSD approach, which includes up to double excited cluster operators [22]. In parallel to the usual CC equations, in EOM-CC theory, excited state wave functions are represented by a linear expansion in the space spanned by all states [22, 35]:

$$\left|\Psi_A\right\rangle = \sum_\mu c_\mu \hat{\tau}_\mu \left|\Psi_{CC}\right\rangle = \exp(\hat{T}) \sum_\mu c_\mu \hat{\tau}_\mu \left|\Psi_0\right\rangle \tag{23}$$

where Ψ_A and Ψ_{CC}, refers to the CC excited and ground states, respectively, Ψ_0 to the HF ground state, and $\hat{T}$ is the linear coupled-cluster excitation operator:

$$\hat{T} = \hat{T}_0 + \hat{T}_1 + \hat{T}_2 + \hat{T}_3 + .. = \sum_{\mu} c_{\mu} \hat{\tau}_{\mu} \tag{24}$$

where c_μ denotes the cluster amplitudes and $\hat{\tau}_\mu$ the excitation operators including none, single, double, triple, and higher-order replacements. These methods use commutation relations to solve the Schrödinger equation for the excited state, and may be regarded as a conventional CI theory in which the configuration expansions carry the information about the excitation structure while a similarity-transformed Hamiltonian carries information about electron correlation [35, 57]. EOM-CC methods in different versions have been also extended to deal with open-shell ground states and compute IPs and EAs [58].

The family of methods CCS, CC2, CCSD, CC3, and CCDST is based on response theory [59]. Poles and residues of the linear-response CC equations yield excitation energies and transition matrix elements. CCS, CCSD, and CCSDT give a complete coupled cluster treatment of single, single-double, and single-double-triple spaces, respectively, for excited states, but just in systems with closed-shell ground states. The CCS approach is equivalent to the single excited configuration interaction or Tamm-Dancoff approach [60]. The iterative hybrid CC2 and CC3 procedures introduce approximations of similar nature although differing in the level of excitation. In this way, in CC2 the doubles of the CCSD approach and in CC3 the triples of the CCSDT approach are approximated by using perturbation theory up to first- and second-order, respectively. In this way, for instance, the CC3 wavefuntion is obtained as [35]:

$$|\Psi_{CC3}\rangle = \exp(\hat{T}_1 + \hat{T}_2 + \hat{Q}_3)|\Psi_0\rangle \tag{25}$$

where Ψ_0 refers to the HF reference, and the $\hat{T}$ operators include the single and double excitation cluster operators, while the effect of the triple excitations are introduced by the $\hat{Q}$ operators iteratively. CC3 include the single and double excitations at third order and the triple excitations at second order in the fluctuation potential, all of them one order higher than CCSD. This approximate way to include higher excitation levels allows less demanding computational procedures, scaling N^{4-7} from CCS to CC3, respectively [23, 60].

In order to get accurate excitation energies and properties, the single-configuration coupled-cluster methods should include high excitation levels to compensate both the poor reference wave function and the multiconfigurational character of the excited states. In situations where the HF reference is good enough, CC-based methods are, up-to-date and in practice, the most accurate methods to compute excited states in small to medium size molecules with closed-shell ground states, but only for those states which are well described by singly excited configurations and in systems were the ground state has a clear single-configuration character. In those cases, and in order to get accuracy better than typical

propagator or TD-DFT methods, triple excitations have to be included in the cluster expansion. Approaches valid for practical cases are, in general, EOM-CCSD(T) and CC3, while those only including double excitations as SAC-CI, EOM-CCSD or CC2, can be considered of lower quality than, for instance, multireference perturbation methods such as CASPT2 or similar approaches [15–18, 52, 61-63]. The precision of the CC methods decreases in systems with open-shell ground states. Less accurate is the behavior of the methods when the character of the states is clearly multiconfigurational. For instance, the mentioned 2^1A_g state of polyenes, a multiconfigurational state with a large contribution of doubly excited configurations in the CASSCF description, is a good example. The CASPT2 vertical result, 6.27 eV, can be considered here a good benchmark, because the CASPT2 method has proved its accuracy on matching the experimental two-photon value for the analogous state in hexatriene [42]. EOM-CCSD, CCSD(T), and CCSD($\widetilde{T}$), the latter a non-iterative version for the inclusion of triple excitations, deviate 1.0, 0.7, and 0.5 eV from the CASPT2 value, respectively [62]. Other example shows up in the 1^1E_{1g} state of ferrocene, with an error of 1.5 eV from experiment at the CC2 level [61]. More dramatic is the situation in other systems, in which the excited state is clearly multiconfigurational, where not even the inclusion of triple excitations can lead to accurate results. For instance, the EOM-CCSD description of the 2^1A_1 state of ozone leads to huge errors, 5-6 eV, that approximate inclusion of triple excitations cannot solve [54]. A similar situation occurs for some excited states of C_2, showing deviations with respect to FCI of 2.05, 0.86, and 0.41 eV at the EOM-CCSD, CC3, and EOM-CCSDT levels [54], the second and third CC methods differing in the perturbative or variational procedure to include triple excitations. For the description of the states of the NO dimer, N_2O_2, EOM-CCSD fails on describing even the ground state, and EOM-CCSDT shows large inaccuracies to describe the excited states [53]. The inclusion of quadruple excitations, unpractical so far, would improve some of those results, but the only solution in prospect to beat in accuracy the lower level and less expensive multireference perturbation approaches such as CASPT2, is to use multireference coupled-cluster (MRCC) methods [64], in which the required excitation level will be certainly lower.

Additionally to the calculation of energy eigenvalues, molecular properties for the different electronic states, and transition properties must be computed to define the spectroscopy of a molecular system. Properties such as the electric dipole moment, the frequency-dependent polarizability tensor, the nuclear magnetic shielding tensor, among others, are intrinsic properties of the system responsible of many spectroscopic and even structural phenomena whose calculation require also accurate *ab initio* approaches. If we focus on the molecular electromagnetic properties, they can be derived either as derivatives of the electronic energy or as derivatives of molecular electromagnetic moments and fields [65]. In non-variationally optimized wave functions, the Hellmann-Feynman theorem is not satisfied and the properties obtained as derivatives of the energy do not agree with the expectation values of the properties. This is the case, in general, of CC or MP approaches, which should be preferred in order to get results including most of correlation energy, although, in many cases, MCSCF properties can be considered reasonable [15–18]. Redefinitions of the expectation values in high-level methods have to be performed. Most *ab*

initio methods used to compute properties can be divided in three types: (1) those which evaluate properties by approximations to exact perturbation theory, such as the sum-over-states (SOS) procedures and the polarization propagator methods, RPA, SOPPA or MCRPA; (2) those which use perturbation theory with approximate wave functions, such as the Coupled Hartree-Fock (CHF) method or the response methods using different wave functions, in particular MCSCF or coupled-cluster, and (3) the derivative-based methods, where numerical or analytical evaluation of the derivatives of the electronic energy or properties in the presence of the perturbing field is performed, for instance, by finite field approaches. A comprehensive review can be found elsewhere [65]. Also, transition properties, such as transition multipole moments needed to obtain intensities, transition probabilities and radiative lifetimes and kinetic constants, have been computed at different levels, although the response approaches are becoming common to get accurate results.

Finally, we shall comment and summarize advantages and disadvantages of the mentioned methods. Of course, it reflects our own opinion on the subject. Here we have not included all methods available or developed, just those more widely used. Nowadays (2004) single-configuration *ab initio* methods are useful to describe excitation energies, excited state properties, and transition probabilities, always subordinated to certain restrictions. CIS-derived methods cannot be recommended in practically any situation. A low-level general description of the excited states structure can be better obtained by means of carefully calibrated TD-DFT methods (the mixed and empirically corrected DFT/MRCI approach can be considered the best) [66], provided that the limitations of the DFT approaches and their low accuracy are well known. Regarding the propagator methods, they have, as the other methods of this section, the advantage of being (only partially) black-box approaches, and, therefore, they can be used also to get a qualitative picture of the spectrum, although neither all states nor all systems. Finally, coupled-cluster based approaches, assume that the effect of triple excitations are included, yield an accurate account of many states and systems, but not all of them. Regarding molecular and transition properties, the CC-based methods are surely the most accurate procedures available, provided that the approach is appropriate, although they are computationally more demanding and further improvements in their performance are necessary. In order to have an overall accurate description of all types of excited states, it is necessary to point out that, at present, the multireference perturbative methods, with CASPT2 as the most widely used approach [15–18], represents the only generally applicable method for the calculation of excited states, in all type of molecular systems, closed- and open-shells, multiconfigurational and degenerated situations, dissociations, etc [35]. It can be expected that in the near future, the multiconfigurational coupled-cluster approaches reach the maturity to be of practical use in molecular systems of reasonable size, and then, higher accuracy will be available in all cases. The full development of the methods will require also the implementation of geometry optimizers, reaction paths algorithms, etc, and some years will pass until all the needed tools become available. Up-to-date, analytical gradients for excited states in single-configuration methods are available, at a high computational cost, at the SAC-CI [67], EOM-CCSD [68], and CC2 [69] levels.

4.2. Multiconfigurational methods

Let us considered the wave function of CI type

$$|\Psi\rangle = \sum_{m} c_m |m\rangle \tag{26}$$

expanded in a many-electron basis set of determinants. As in the H_2 molecule, one can select a number of determinants to describe the correct dissociation limit. When the energy is minimized with respect to the coefficients of the expansion we are using the configuration interaction (CI) method. It should be kept in mind that actual calculations are performed using either spin-adapted CSFs or determinants. In case that the expansion contains more than one configuration, the process is denoted as multireference CI (MRCI). The wave function of Eq. (26) is a multireference function and, at least, the singly and doubly excited determinants generated from each reference determinant $|m\rangle$ are taken into account. When the reference wave function consists of a single configuration, such as a closed-shell HF wave function, we are in the framework of single-reference CI wave functions, *e.g.*, SDCI (singly and doubly excited CI). Including up to N-tuply excited determinants Eq. (26) would represent the full CI wave function. A comprehensive discussion on the distinct types of the MRCI method, including technical aspects on its efficient implementation, can be found elsewhere [14].

Coming back to Eq. (26), the MCSCF energy is obtained by minimizing $\langle\Psi|\hat{H}|\Psi\rangle$ to determine both the optimum CI expansion coefficients (as in the CI method) and the optimum form of the orbitals used to build $|m\rangle$. The orbital optimization is similar to that carried out in the HF SCF method, therefore the approach is known as the multiconfigurational self-consistent field (MCSCF). The MCSCF energy is usually expressed within the second-quantization formalism [35, 46]. The electronic Hamiltonian given in Eq. (2), has the following expression (physicists' notation) [1] in second quantization

$$\hat{H} = \sum_{ij} \langle i|\hat{h}|j\rangle \, \hat{a}_i^\dagger \hat{a}_j + \frac{1}{2} \sum_{ijkl} \langle ij|kl\rangle \, \hat{a}_i^\dagger \hat{a}_j^\dagger \hat{a}_l \hat{a}_k \tag{27}$$

where the sums run over the set of spin orbitals, and $\hat{a}_i^\dagger$ and $\hat{a}_i$ are the creation and annihilation operators, respectively. In the notation often referred to as the chemists' notation, the Hamiltonian is expressed has the form

$$\hat{H} = \sum_{ij} [i|\hat{h}|j] \, \hat{a}_i^\dagger \hat{a}_j + \frac{1}{2} \sum_{ijkl} [ij|kl] \, \hat{a}_i^\dagger \hat{a}_k^\dagger \hat{a}_l \hat{a}_j \tag{28}$$

Summing over the spin leads to

$$\hat{H} = \sum_{ij} (i|\hat{h}|j) \, \hat{E}_{ij} + \frac{1}{2} \sum_{ijkl} (ij|kl) \, (\hat{E}_{ij}\hat{E}_{kl} - \delta_{jk}\hat{E}_{il}) \tag{29}$$

$$\hat{H} = \sum_{ij} h_{ij} \hat{E}_{ij} + \frac{1}{2} \sum_{ijkl} g_{ijkl} \left(\hat{E}_{ij} \hat{E}_{kl} - \delta_{jk} \hat{E}_{il} \right) \tag{30}$$

where the sums run over the molecular orbitals and the spin summed excitation operators, $\hat{E}_{ij}$, defined as

$$\hat{E}_{ij} = \sum_{\sigma=\alpha,\beta} \hat{a}^{\dagger}_{i\sigma} \hat{a}_{j\sigma} = \hat{a}^{\dagger}_{i\alpha} \hat{a}_{j\alpha} + \hat{a}^{\dagger}_{i\beta} \hat{a}_{j\beta} \tag{31}$$

have also been introduced. In Eq. (30) the elements h_{ij} include the kinetic energy for electrons and nucleus-to-electron attraction; the two-electron integrals involving the molecular orbitals, in chemists' notation, are denoted by g_{ijkl}.

Given the wave function (26) as linear combination of a finite set of determinants, the expectation value of the Hamitonian is

$$E = \langle \Psi | \hat{H} | \Psi \rangle = \sum_{ij} h_{ij} \sum_{mn} c^{*}_{m} \langle m | \hat{E}_{ij} | n \rangle c_{n} + \frac{1}{2} \sum_{ijkl} g_{ijkl} \sum_{mn} c^{*}_{m} \langle m | \hat{E}_{ij} \hat{E}_{kl} - \delta_{jk} \hat{E}_{il} | n \rangle c_{n} =$$

$$= \sum_{ij} h_{ij} \sum_{mn} c^{*}_{m} D^{mn}_{ij} c_{n} + \sum_{ijkl} g_{ijkl} \sum_{mn} c^{*}_{m} P^{mn}_{ijkl} c_{n} =$$

$$= \sum_{ij} h_{ij} D_{ij} + \sum_{ijkl} g_{ijkl} P_{ijkl} \tag{32}$$

being

$D^{mn}_{ij} = \langle m | \hat{E}_{ij} | n \rangle$, one-electron coupling coefficients. Their possible values are –1, 0, 1, 2 in a many-electron basis set of Slater determinants,

$P^{mn}_{ijkl} = \frac{1}{2} \langle m | \hat{E}_{ij} \hat{E}_{kl} - \delta_{jk} \hat{E}_{il} | n \rangle$, two-electron coupling coefficients,

$D_{ij} = \sum_{mn} c^{*}_{m} D^{mn}_{ij} c_{n}$, element of the first-order reduced density matrix,

$P_{ijkl} = \sum_{mn} c^{*}_{m} P^{mn}_{ijkl} c_{n}$, element of the second-order reduced density matrix.

The expression for the energy (32) gives the clue for derivation of optimization algorithms employed in the MCSCF methods. It worth noting that information about the MOs is entirely contained in the one- and two-electron integrals, whereas the CI coefficients are involved in the matrices **D** and **P**. Thus, the parameters to be varied are the CI coefficients and the MOs, which is made by considering their variations as rotations within an orthonormalized vector space. Since the exponential of an anti-Hermitian matrix is the most general expression of a unitary matrix, the rotations in the MCSCF optimization procedure are done by using that

type of matrices. There are several techniques to carry out such a process. MCSCF optimization methods can be classified as first-order and second-order methods, depending on the convergence type. A first-order treatment is only based in the computation of the energy and the first derivatives of the energy with respect to the variational parameters. The second-order MCSCF methods are based on an energy expansion up to second order and the second derivatives of the energy are also computed. They are characterized by a quadratic convergence in the final steps of the optimization procedure. The Newton-Raphson approximation up to second order, where the energy is expanded in a Taylor series as function of the variational parameters, is probably the most prominent algorithm. The new values for the parameters are obtained by solving a set of linear equations. The convergence process is rapid and efficient in the proximities of the final solution (quadratic convergence), although the trust region is usually small. It is the standard optimization method and most of the remaining approaches can be related to it either as modified or simplified algorithms. Details on the particular techniques can be found in the specialized literature [28, 35, 70].

From a practical point of view, the selection of a particular algorithm would depend on the necessities of the application at hand. An advantage of a second-order algorithm is that the stationary point is characterized, that is, the condition of minimum can be established. Comparatively, in a second-order method a full iteration is more time consuming as compared to simplified approaches, although the number of iterations required to converge are relatively smaller. One has to balance the advantages and disadvantages in the two type of approaches prior utilizing one of them in a particular study. Anyway, because of the computational resources available today, one can freely take the decision of enjoying the advantages of both. Independently of the chosen algorithm, it is highly recommended to supply the MCSCF optimization calculation with good starting orbitals, in accordance with the physics of the problem to elucidate. Otherwise, unwanted solutions might easily come out of the calculation, which are simply nonsense.

We have assumed that the N-electron basis set is constituted by Slater determinants. Nevertheless, the Hamiltonian operator, as well as the orbital rotations, can be expressed as function of the orbital excitation operators, which commute with the spin operators. It is, therefore, possible to work entirely in a N-electron basis set formed by spin-adapted CSFs. There are many manners to build eigenvectors of the spin operators from Slater determinants. Among them the graphical unitary group approach (GUGA) has played an outstanding role. Indeed, the excitation operators fulfill the same commutation relationships as the generators of the unitary group of dimension n, and for that reason the $\hat{E}_{ij}$ operators are often referred as to generators. A CSFs basis set leads to shorter CI expansions that a basis set of Slater determinants, but the CI algorithms employing determinants are more efficient. The issue was in the past a subject of great debate. A certain consensus has been reached today, which is reflected in available software [71], making practical use of the advantages of both types of N-electron basis sets.

As stated above, the CASSCF method [72] is probably the MCSCF method more widely used at present. In the CASSCF method, the orbitals are classified in three categories, depending on the role they play in building the many-electron wave function: inactive, active, and secondary orbitals. Inactive and active orbitals are occupied in the wave functions, whereas the remaining of the orbital space, given by the size of the one-electron basis set employed, is constituted by secondary orbitals, also called external or virtual. Inactive orbitals are doubly occupied in all the CASSCF configurations. The number of electrons occupying inactive orbitals is, therefore, twice the number of inactive orbitals. The rest of the electrons (called active electrons) occupy active orbitals. The CASSCF wave function is formed by a linear combination of all the possible configurations that can be built by distributing the active electrons among the active orbitals and are consistent with a given spatial and spin symmetry. That is, in the configuration space spanned by the active orbitals, the CASSCF function is complete (or full). Inactive orbitals are also optimized in the variational process but they are treated as in the restricted HF function. The CASSCF energy is invariant to rotations among the active orbitals.

Several states that belong to a same symmetry are usually computed by means of a State-Average (SA) CASSCF calculation, where a functional of energy is defined as average of a number of states (I=1, M)

$$E_{average} = \sum_{I} \omega_I E_I \qquad (33)$$

being ω_I the factors of the relative weight for each state considered. From a SA-CASSCF calculation comes out a set of average orbitals and a number of orthogonal wave functions equal to the number of roots used in the average process. In this manner, it is sometimes possible to overcome the problem of "root flipping", the interchange of roots along the CASSCF optimization procedure. For a given spatial and spin symmetry, the treatment of excited states is preferably performed by using SA-CASSCF calculations. In principle, it is also possible to make a single CASSCF calculation for higher roots (I > 1), optimizing just one state. Nevertheless, experience shows that in most cases, it can only be achieved for I=2, the second root of a given irreducible representation.

The active space provided by the user of a CASSCF software represents a key point to obtain accurate theoretical predictions, once that dynamic correlation has subsequently been taken into account, for instance at the CASPT2 level. The properties of a CASSCF wave function depend on the active space. Thus, a valence CASSCF is size-extensive and the corresponding CASPT2 results become also nearly size-extensive (formally the CASPT2 method is not size-extensive). As in any quantum-chemical approach one has to make sure that the method has enough flexibility to describe the chemical process under consideration. The flexibility in a CASSCF wave function is determined by the active space.

The CASPT2 method can be seen as a conventional non-degenerate perturbation theory, that is, a single reference function is considered, with the particularity that such reference function (zeroth-order wave function) is a CASSCF wave function and uses internal contraction in its formulation. The solution to the equation

$$\hat{H}(\lambda)\Psi(\lambda) = E(\lambda)\Psi(\lambda) \tag{34}$$

is expanded in power series of λ:

$$\hat{H}(\lambda) = \hat{H}^{o} + \lambda\hat{H}' \tag{35}$$

$$\Psi(\lambda) = \Psi^{(o)} + \lambda\Psi^{(1)} + \lambda^2\Psi^{(2)} + \cdots \tag{36}$$

$$E(\lambda) = E^{(o)} + \lambda E^{(1)} + \lambda^2 E^{(2)} + \cdots \tag{37}$$

Correction of order k to the wave function, $\Psi^{(k)}$, and to the energy, $E^{(k)}$, are obtained by solving consecutively the corresponding perturbation equations, which have the following generic form

$$(\hat{H}^{o} - E^{(o)})\,\Psi^{(k)} = -\hat{H}'\,\Psi^{(k-1)} + \sum_{j=0}^{k-1} E^{(k-1)}\,\Psi^{(j)} \qquad (k \neq 0) \tag{38}$$

where the energy correction to order k, using intermediate normalization, is

$$E^{(k)} = \left\langle \Psi^{(o)} \middle| \hat{H}' \middle| \Psi^{(k-1)} \right\rangle \tag{39}$$

Therefore, we can write

$$E^{(1)} = \left\langle \Psi^{(o)} \middle| \hat{H}' \middle| \Psi^{(o)} \right\rangle \tag{40}$$

$$E^{(2)} = \left\langle \Psi^{(o)} \middle| \hat{H}' \middle| \Psi^{(1)} \right\rangle \tag{41}$$

The first-order correction to the wave function is given by

$$\Psi^{(1)} = \hat{R}^{(o)}(E^{(1)} - \hat{H}') \left| \Psi^{(o)} \right\rangle \tag{42}$$

with $\hat{R}^{(o)}$ being the reduced resolvent

$$\hat{R}^{(o)} = \left(1 - \left| \Psi^{(o)} \right\rangle \left\langle \Psi^{(o)} \right|\right)\left(\hat{H}^{o} - E^{(o)}\right)^{-1} \tag{43}$$

The set of functions required to compute the first-order correction of the wave function, $\Psi^{(1)}$, is formed by those that interact with the zeroth-order wave function through the Hamiltonian in the perturbation theory of Rayleigh-Schrödinger, and it is known as the *first-order interacting space* [73]. Taking into account the one and two particle nature of the Hamiltonian, the first-order interaction space, called hereafter V_{SD}, comprises the functions generated by singly and doubly excited configurations from the zeroth-order wave function. In the CASPT2 formulation, the V_{SD} space is divided in eight subsets, according to the nature of the excited configurations (see details in Ref. [10]). The corresponding functions are built by applying products of excitation operators, E_{pq} E_{rs}, to the zeroth-order wave function $|o\rangle$, Eq. (26), with the coefficients c_m kept as determined in the CASSCF wave function. It is the reason why the CASPT2 method is internally contracted. In non-contracted methods [13, 14], the excitation operators act directly on the functions $|m\rangle$ of the linear combination described by Eq. (26). Both singly and doubly replacements from the CASSCF wave function are considered. The singly excited configurations can be explicitly seen as linear combinations of certain products of excitation operators. Internal contraction makes the perturbation series considerably shorter, without affecting significantly the quality of the results [10]. Nevertheless, although the dimension of the first-order interacting space is considerably smaller because of the internal contraction, the complexity to obtain the first-order wave function increases because the resulting functions belonging to V_{SD} are not in general orthogonal and may also have linear dependencies.

The first-order correction of the wave functions is expanded in the basis of the functions $|j\rangle$ belonging to the V_{SD} space

$$\Psi^{(1)} = \sum_{j=1}^{M} C_j |j\rangle \qquad M \geq \dim V_{SD} \tag{44}$$

The coefficients $\{C_j, j = 1, ..., M\}$ are obtained from the system of linear equations

$$\sum_{j=1}^{M} C_j \langle i|\hat{H}^o - E^{(o)}|j\rangle = -\langle i|\hat{H}'|o\rangle \qquad i = 1, ...M \tag{45}$$

where $E^{(o)} = \langle o|\hat{H}^o|o\rangle$ is the zeroth-order wave function and must be solved iteratively. In standard CASPT2, the zeroth-order Hamiltonian is expressed in terms of a generalized Fock operator, which can be written as a sum of a diagonal, $\hat{F}_D$, and non-diagonal, $\hat{F}_N$, contributions

$$\hat{F}_T = \hat{F}_D + \hat{F}_N \tag{46}$$

The operator is defined in such way that for a closed-shell HF reference wave function is equivalent to the Møller-Plesset Hamiltonian. For multiconfigurational single-reference perturbation theory, the choice of the zeroth-order Hamiltonian is not unique and it has been

the subject of active research and discussions yielding a number of different successful variants [16].

Eq. (45) can then be rewritten as

$$\sum_{j=1}^{M} C_j \langle i|\hat{F}_T - E^{(o)}|j\rangle = -\langle i|\hat{H}'|o\rangle \qquad i = 1, ...M \tag{47}$$

In order to simplify the notation, the following matrices and vectors are introduced

$$(\hat{F}_X)_{ij} = \langle i|\hat{F}_X|j\rangle \qquad X = D, N \tag{48}$$

$$S_{ij} = \langle i|j\rangle \tag{49}$$

$$V_i = \langle i|\hat{H}|o\rangle \tag{50}$$

where i, j = 1, ...M. The column vector **C** contains the coefficients C_j of the expansion. The difficulties in the resolution of Eq. (47) depend on the choice of the one-particle operator. In the simplest case, using $\hat{F}_D$, it leads to

$$[\mathbf{F}_D - E^{(o)}\mathbf{S}]\mathbf{C} = -\mathbf{V} \tag{51}$$

and the second-order correction to the energy comes out as the product of $\mathbf{V}^\dagger\mathbf{C}$. In most cases $M \geq \dim V_{SD}$ and the linear dependences have to be removed. It is done by diagonalizing the overlap matrix **S** and discarding the eigenvectors with eigenvalues equal (or close) to zero. The resulting vectors are then orthogonalized and a subsequent diagonalization of the Fock matrix written in the orthogonal basis takes place. The $E^{(2)}$ correction is easily evaluated as function of the transformed matrices. The process becomes much more elaborated when the full operator $\hat{F}_T$ is used [10]. It is the recommended procedure.

The normalized wave function corrected up to first order is given by

$$|\Psi\rangle = C_o|o\rangle + C_1|\Psi^{(1)}\rangle \tag{52}$$

with $C_o^2 + C_1^2 = 1$. The weight of the reference function (C_o^2) can be used as a simple and rapid criterion of quality for the perturbation treatment carried out. Ideally, in order to get a fast convergence in the perturbation series, the weight should be close to unity. Nevertheless, its value depends on the number of correlated electrons [28]. Thus, upon enlarging the molecular system the reference weight decreases. The electronic excited states considered should have a similar magnitude for the weight as compared to the ground state, employing the same active space. Sometimes intruder states appear in the second-order calculation, which are normally related to the occurrence of large coefficients in the first-order expansion, leading to a low

value for the reference weight. Analysis of the states with large coefficients (intruder sates) may give a hint about the type of reformulation in the perturbation partition necessary to overcome the problem. Thus, a new CASSCF calculation might be designed comprising in the active space the orbitals implied in the description of the previous intruder states. It is the proper action to be taken when intruder states are strongly interacting with the CASSCF reference wave function, with contribution to the second-order energy larger than 0.1 au, because it points out to obvious deficiencies in the choice of the active space. Intruder states are often present in the treatment of excited states of small organic compounds when the active space does not include the full π valence system. Thus, the low weight for the zeroth-order wave function in such a case just tells us that the active space has to be enlarged in a way that previous intruder states would be treated variationally, that is, they should be moved to the CAS-CI space. It is also frequent to find calculations where the reference weight of the excited state is "somewhat low" compared to that of the ground state, but a particular state cannot be identified as intruder in the first-order wave function, which is instead characterized by a large number of low-energy minor contributions. It occurs often in the simultaneous computation of valence and Rydberg states, where the one-electron valence basis set has been augmented with Rydberg-type functions. We have to face then accidental near-degeneracy effects, implying weakly interacting intruder states, and the level-shift (LS) technique is especially useful in order to check the validity of the perturbation treatment performed. Many times one has to apply both strategies: enlargement of the active space to overcome the problem of severe intruder states, and, with the enlarged active space, the LS technique is applied in order to minimize the effect of weak interacting intruder states.

The level-shift CASPT2 (LS-CASPT2) method removes efficiently weak intruder states by the addition of a shift parameter, ε, to the zeroth-order Hamiltonian and a subsequent back correction of its effect to the second-order energy [16, 28, 74]. It can be shown that the corrected level-shift second-order energy, $E_{LS}^{(2)}$, is equal to the standard CASPT2 energy, $E^{(2)}$, in first order of ε

$$E^{(2)} \approx \widetilde{E}^{(2)} - \varepsilon\left(\frac{1}{\widetilde{\omega}} - 1\right) \equiv E_{LS}^{(2)} \tag{53}$$

where $\widetilde{E}^{(2)}$ and $\widetilde{\omega}$ (weight of the CASSCF wave function) were obtained by using the shifted Hamiltonian. The relationship (53) might not be valid when intruder states appear in the first-order interacting space. It is highly recommended to make an analysis of the trends for the weights ω, total, and excitation energies upon varying the values of ε. For instance, results at ε = 0.0 (standard CASPT2), 0.1, 0.2, 0.3, 0.4 au are sufficient to establish the proper behavior of the LS-CASPT2 results. It is extremely dangerous to rely on just one result, because the appearance of an accidental near degeneracy might lead to large errors in the excitation energies. In order to demonstrate the proper performance of the LS-CASPT2 technique, calibration calculations of that type always have to be carried out. The best choice for ε is the lowest possible value capable of removing intruder states. In the absence of intruder states the $E_{LS}^{(2)}$ energy varies only slightly with respect to the value of ε. As can be seen, in this type of

approaches there is a large interaction researcher-software. The responsibility for the decisions taken along the computational process belongs, of course, to the user (researcher) of the tool (program). Other formulations of the multireference perturbation theory have been developed although they have not widespread use [75–80].

The multi-state CASPT2 (MS-CASPT2) [81, 82] procedure represents an extension of the CASPT2 method for the perturbation treatment of chemical situations that require two or more reference states. For instance, situations such as avoided crossings and near-degeneracy of valence and Rydberg states, which cannot be fully accounted for by just using a single-reference perturbation treatment.

In the MS-CASPT2 method an effective Hamiltonian matrix is constructed where the diagonal elements correspond to the CASPT2 energies and the off-diagonal elements introduce the coupling up to second order in the dynamic correlation energy. Let us assume that we have performed two CASPT2 calculations for the corresponding reference wave functions Φ_i (i=1, 2), obtained by using average CASSCF for those two roots and a set of average molecular orbitals is, therefore, available. In order to build the matrix representation of the Hamiltonian using as basis set the two normalized wave functions corrected up to first order, $\Psi_i = \Phi_i + \Psi_i^{(1)}$, the following matrices are defined:

$$S_{ij} = \left\langle \Psi_i \middle| \Psi_j \right\rangle = \left\langle \Phi_i + \Psi_i^{(1)} \middle| \Phi_j + \Psi_j^{(1)} \right\rangle = \delta_{ij} + s_{ij} \tag{54}$$

$$\left\langle \Phi_i \middle| \hat{H} \middle| \Phi_j \right\rangle = \delta_{ij} E_i \tag{55}$$

$$\left\langle \Phi_i \middle| \hat{H} \middle| \Psi_j^{(1)} \right\rangle = e_{ij} \tag{56}$$

Notice that the two wave functions are not orthogonal, since $\left\langle \Phi_i \middle| \Phi_j \right\rangle = \delta_{ij}$ and $\left\langle \Phi_i \middle| \Psi_j^{(1)} \right\rangle = 0$, but $\left\langle \Psi_i^{(1)} \middle| \Psi_j^{(1)} \right\rangle = s_{ij}$. On the other hand, the CASSCF energy for state *ith* is represented by E_i and the elements e_{ij} are the CASPT2 correlation energies. For each state, the Hamiltonian can be expressed as the sum of a zeroth-order contribution and a Hamiltonian taking care of the remaining effects

$$\hat{H} = \hat{H}_i^o + \hat{H}_i' \tag{57}$$

Therefore, up to second order it holds true that

$$\left\langle \Psi_i^{(1)} \middle| \hat{H} \middle| \Psi_j^{(1)} \right\rangle \approx \left\langle \Psi_i^{(1)} \middle| \hat{H}_i^o \middle| \Psi_j^{(1)} \right\rangle \approx \left\langle \Psi_i^{(1)} \middle| \hat{H}_j^o \middle| \Psi_j^{(1)} \right\rangle \tag{58}$$

The elements $\left\langle \Psi_i^{(1)} \middle| \hat{H}_i' \middle| \Psi_j^{(1)} \right\rangle$ correspond to third order corrections and, consequently, they are not considered. The matrix representation of the Hamiltonian is not symmetric $H_{12} \neq H_{21}$.

Assuming that the off-diagonal terms are very similar, as it is implicit from Eq. (58), the matrix is made symmetric by using the average value

$$\left\langle \Psi_i^{(1)} \left| \hat{H} \right| \Psi_j^{(1)} \right\rangle = \frac{1}{2}\left(\left\langle \Psi_i^{(1)} \left| \hat{H}_i^o \right| \Psi_j^{(1)} \right\rangle + \left\langle \Psi_i^{(1)} \left| \hat{H}_j^o \right| \Psi_j^{(1)} \right\rangle \right) \tag{59}$$

The matrix element including zeroth-, first-, and second-order corrections takes the general form

$$\hat{H}_{ij} = \left\langle \Psi_i \left| \hat{H} \right| \Psi_j \right\rangle = \delta_{ij} E_i + \frac{1}{2}(e_{ij} + e_{ji}) + \frac{1}{2}(E_i^{(o)} + E_j^{(o)})\, s_{ij} \tag{60}$$

By solving the corresponding secular equation $(\mathbf{H}-E\mathbf{S})\mathbf{C}=0$, the eigenfunctions and eigenvalues can be obtained. They correspond to the MS-CASPT2 wave functions and energies, respectively.

The MS-CASPT2 wave function can be finally written as

$$\Psi_p = \sum_i C_{pi} \left| i \right\rangle + \Psi_p^{(1)} = \left| i_p \right\rangle + \Psi_p^{(1)} \tag{61}$$

where $\left| i \right\rangle$ are the CASSCF reference functions and $\Psi_p^{(1)}$ is the first-order wave function for state *p*. Accordingly, the function formed by a linear combination of the CAS states involved in the MS-CASPT2 calculation is the model state and can be considered as a new reference function for state *p*. This reference function is the so-called Perturbation Modified CAS (PMCAS) [82]. It is used for the computation of transition properties and expectation values at the MS-CASPT2 level.

For the proper use of the MS-CASPT2 method, the condition (58) has to be fulfilled. In practice, it means that the asymmetric effective Hamiltonian matrix should have small and similar off-diagonal elements. Otherwise, the average process carried out, $(H_{12}+H_{21})/2$, may lead to unphysical results, in both the MS-CASPT2 energies and eigenfunctions. The condition that $H_{12} \cong H_{21}$ can be achieved by enlarging the active space, which implies a redefinition of the zeroth-order Hamiltonian. Large active spaces, beyond the main valence MOs, are used naturally in the simultaneous treatment of valence and Rydberg states, where the MS-CASPT2 approach has proved to be extremely useful. Especial caution has to be exercised, however, for the computation of a crossing point between two surfaces, as in the case of conical intersections (and avoided crossings), crucial in photochemistry.

The states involved in a conical intersection have usually different nature. Quite often one state has covalent character, whereas the other is zwitterionic [83]. They are described by hole-hole and hole-pair VB structure, respectively. The effect of dynamic correlation is usually much more pronounced for zwitterionic than for covalent states. As a result, with

moderate (valence) active spaces, the off-diagonal elements become very different, because the covalent state is comparatively described more accurate than the zwitterionic state. Active spaces comprising MOs beyond the valence shell would be required to make $H_{12} \cong H_{21}$. In addition, the structure of the 2x2 effective Hamiltonian is

$$H^{eff} = \begin{pmatrix} H_{11} & H_{12} \\ H_{21} & H_{22} \end{pmatrix} \approx \begin{pmatrix} E_1^{PT2} & \Delta \\ \Delta & E_2^{PT2} \end{pmatrix} \tag{62}$$

where $E_1^{PT2} = E_1 + e_{11}$ and $E_2^{PT2} = E_2 + e_{22}$ are the CASPT2 energies of the two states and $\Delta = (H_{12} + H_{21})/2$. If the states are degenerate at the CASPT2 level, $E_1^{PT2} = E_2^{PT2} = E$, and the multi-state energies and wave functions are

$$E_{\pm} = E \pm \Delta \tag{63}$$

$$\Psi_{\pm} = \frac{1}{\sqrt{2}}(\Psi_1 \pm \Psi_2) \tag{64}$$

As $\Delta = 0$ the MS-CASPT2 and the CASPT2 solutions are equivalent, what is expected to occur at the conical intersection. Therefore, by providing enough flexibility to the active space, one has to make sure that the condition $H_{12} \cong H_{21}$ is satisfied and Δ becomes small ($\leq$ 2 kcal/mol). As a conclusion, computation of surface crossings at the MS-CASPT2 level (so far numerically) is expected to require more extended active spaces than those done at the CASSCF level. What does it happen if Δ is larger than 2 kcal/mol? For systems of large molecular size one cannot be sure whether that result points out to the presence of an avoided crossing or it is just spurious because of the limited active space employed. As shall be illustrated in Section 6, dynamic correlation plays sometimes a crucial role in determining the nature of the lowest surface crossings. Nevertheless, except for small molecular systems, the MS-CASPT2 approach in its present formulation does not represent a practical solution for this purpose. Methodological efforts are certainly required to improve the present situation. In this respect, recent advances on analytic energy gradients for general MRPT methods seem very promising [84]. On the order hand, computation of conical intersections at the CASPT2 level uses two non-orthogonal wave functions and how it might affect to the structure of the singular point so obtained is not yet known. Unfortunately, localization of conical intersections including dynamic correlation by using variational strategies, at the MRCI level for instance, is currently limited to small-size molecular systems [85-87].

5. EXCITED STATES AND SPECTROSCOPY

5.1. General Considerations

Quantum-chemical methods provide information for excited states directly applicable to explain and predict the spectroscopy of molecular systems. A balanced description of the different electronic states is required in order to obtain the basic data, that is, energy

differences and transition probabilities, in an accurate way. This goal is a much more difficult task for excited states as compared to the ground state. First, one has to deal with many classes of excited states, each one requiring different amounts of electronic correlation and flexible one-electron basis functions able to describe all effects simultaneously. Then, it is necessary to compute extremely complicated potential energy hypersurfaces where the number of minima, transition states, and surface crossings such conical intersections, is multiplied. Because of the inherent complexity of the problems, the methods and algorithms to compute excited states are not so efficient as for ground states or are still under development [2,4].

The selection of the proper one-electron basis set is the first decision a quantum-chemist has to take in order to plan a calculation, and will determine the accuracy of the obtained results. In general, excited state quantum-chemical calculations require the use of large, diffuse, and flexible basis sets, able to describe at the same level states of compact nature, such as valence, and diffuse, such as Rydberg or anionic states. Atomic Natural Orbital (ANO) basis sets supplemented with diffuse functions or augmented correlation-consistent basis sets (aug-cc-pVXZ, with X=D,T,Q,...), are the best general choice in order to get all type of excited states in the different regions of the spectrum [88]. Because of their balanced construction, ANO basis sets usually get better results with less number of functions than other sets. In a typical calculation in electronic spectroscopy for a medium-size molecule, an ANO contraction of the triple-zeta plus polarization type has been shown to give accurate and reliable results for valence states [15–17]. Specific diffuse functions with small Gaussian exponents, whether distributed on the atomic centers or centred in the molecule, are required to compute Rydberg and anionic excited states. Basis sets of the type 6-31G* are not as accurate but considerably cheaper. If used, they should be carefully calibrated for the studied problem. They may work in cases where the Rydberg states are not competitive with the valence states in the studied energy region. Normally, a full study including both valence and Rydberg states is required in order to validate the quality of the valence results employing smaller basis sets. It particularly holds true in molecular systems with a strong valence-Rydberg mixing [42, 89].

In order to properly compare to the recorded spectroscopic data [18], the excited states have to be computed at significant points in the potential energy hypersurface (PES), which should be previously located by using appropriate optimization algorithms. At the ground or excited state minima, vertical absorption (E_{VA}) and emission (E_{VE}) energy differences are obtained comparable, within the spirit of the Franck-Condon (FC) principle, to the absorption and emission band maxima, respectively. This is just a convenient approach. In order to identify on theoretical grounds the true maxima, a full determination of the vibrational profile of the electronic transition would have to be performed. The vertical transition is however a quite useful concept. The obtained vertical excitation energies and oscillator strengths, together with properties such as the charge distribution in the different states, multipole moments, etc, give an overall view of the structure of the excited states and electronic transitions, although further refinements are required to achieve higher accuracy. Typical

differences between vertical absorption and band maxima range 0.1-0.2 eV in systems where the excited state structure undergoes small changes as compared to that of the ground state [90].

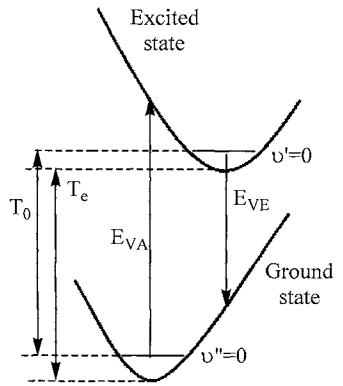

Fig. 1. Computed energy differences describing the molecular photophysics.

In order to gain more spectroscopic insight it is necessary to compute adiabatic transitions, that is, energy differences between states at distinct regions of the PESs [18]. In particular, the energy difference between the excited and the ground state at their respective optimized equilibrium geometries can be related to the electronic band origin, both in absorption and emission. In the former case, it is the smallest possible energy difference allowed in absorption under the assumption that all excitations begin from the relaxed ground state. In emission it is related to the largest energy emitted from the relaxed excited state. As displayed in Fig. 1 such transition is preferably coined T_e. In many cases determination of T_e provides enough information to assign band origins. If more accurate results are needed, the Zero-point Vibrational Energy (ZVE) has to be included in both initial and final states to obtain the vibrational band origin T_0 (also named 0-0 or 0_0^0 transition), which is strictly comparable to the experimental datum (*see* Fig. 1). Usually, determination of the vibrational frequencies (ω_Q) at the state minima is performed within the harmonic approach to simplify the calculations [18]:

$$T_0 = T_e + ZVE_{ij} = T_e + E_{i,vib}(0) - E_{j,vib}(0) = T_e + \tfrac{1}{2}\sum_Q \omega_{i,Q} - \tfrac{1}{2}\sum_Q \omega_{j,Q} \qquad (65)$$

Locating singular points in the hypersurface is a difficult and time-consuming task. It is frequent that geometry optimizations, frequency or property determinations are performed at levels of theory lower than the energy calculations. In most cases it is a question of balance in the results, in particular when highly correlated methods are too expensive for the system under study and low-level approaches have to be employed. For instance, in molecules with double bonds, an enlargement of the bond length is observed when increasing the amount of

correlation energy included. In particular, it has been observed, even for ground states, that in regions with large π delocalization, the difference between methods such as MP2 and CASSCF is quite large (up to 0.03 Å). The former, and the same holds true for DFT, usually overestimates π conjugation [91]. In these cases, π-CASSCF may be a preferable approach to get geometries close to the gas-phase results, because the effects of the π–correlation compensate the lack of σ–correlation. Even more dangerous can be to use crystallographic data. X-ray crystal determinations are known to underestimate double bond lengths (up to 0.02 Å) [92, 93].

Apart from energy differences at specific geometries, spectroscopic determinations require the calculation of transition probabilities in order to get band intensities, emission lifetimes, and kinetic rate constants [94, 95]. Within the static picture and using Fermi's Golden rule, the calculation of transition multipole (dipole approach) moments, together with transition energies, leads to transition probabilities in the form of oscillator strengths:

$$f = \frac{2}{3} E_{VA} M(Q_0)^2 \qquad (66)$$

where E_{VA} is the vertical absorption energy and $M(Q_0)$ is the modulus of the transition dipole moment, computed as the transition dipole components (M_x, M_y, M_z) between the initial and the final state at the ground state equilibrium geometry. The oscillator strength can be directly related to the experimental observation, based on band shapes and half-widths. More precise determinations of band profiles require the calculation of vibronic transition moments and frequencies. From the calculation of transition dipole moments, radiative lifetimes can also be obtained, both in fluorescence and phosphorescence, for the electronic or vibrational states by using the Einstein coefficients (A_{21}) and the Strickler-Berg relationships [95]:

$$A_{21} = \frac{1}{\tau_{rad}} = 2.142005 \cdot 10^{10} M(Q_0)^2 E_{VE}^3 \qquad (67)$$

where τ_{rad} is the radiative lifetime measured in s (the other magnitudes in atomic units) and E_{VE} is the emission maximum, which can be also replaced by T_0. In the case of phosphorescence, the spin-orbit coupling has to be considered to get $M(Q_0)$, which is considerably smaller. Vibronic contributions can be then crucial, in particular in phosphorescence. Intersystem crossing rates can be also obtained in a similar way. In systems including heavy atoms, the spin-orbit coupling can be large enough, the difference between fluorescence and phosphorescence vanishes, and emission is traditionally named luminescence [96].

5.2. On the Valence-Rydberg Mixing: Anti Conformer of *n*-Tetrasilane.

According to the nature of the MOs involved in the description of an electronic state, two basic types of excited states can be found in actual calculations in neutral molecules: valence and Rydberg. The latter have large radial extension of atom-like character, covering the whole

molecule. In a good approximation, a Rydberg state can be described as the result of a one-electron promotion from an occupied orbital to an atom-like orbital of higher quantum number. Therefore, the electron in the Rydberg orbital "feels" the molecule like a cation acting as a point charge, and the presence of the state is justified by the electrostatic interaction between the electron and the cation. In a molecular system formed by atoms of the second period, with electrons of maximum principal quantum number n=2, the Rydberg orbitals begin with n=3, and the Rydberg states 3s, $3p_x$, $3p_y$, $3p_z$, $3d_{x^2-y^2}$, $3d_{z^2}$, $3d_{xz}$, $3d_{yz}$, $3d_{xy}$, are usually found among the lowest Rydberg states, where the promoted electron comes from the HOMO.

Valence and Rydberg states can be characterized by their spatial extent, measured through the expectation values $\langle x^2 \rangle$, $\langle y^2 \rangle$, and $\langle z^2 \rangle$. Valence excited states are described mainly by valence MOs (bonding, lone pairs, and antibonding) and, therefore, they are more compact as compared to diffuse Rydberg states. Comparison of the relative values computed for the second Cartesian moment ($\langle x^2 \rangle$, $\langle y^2 \rangle$, $\langle z^2 \rangle$) can be used as criterion to determine in a simple manner the nature of the excited state; results close to those of the ground state indicate the valence nature of the excited state under consideration. It can be also used to identify a particular type of Rydberg state according to its radial extension. Excited states of intermediate valence-Rydberg nature come out quite often from the computation. To elucidate whether those states actually correspond to spectroscopic states or are just an erroneous consequence of the truncated level of theory employed is not an obvious task and the actions to be taken depend on the particular case. Higher levels of theory are usually required to give a clue in the right direction. Experience shows, however, that valence-Rydberg mixing found in vertical transitions is in most cases spurious and it progressively vanishes upon the increasing level in the treatment of dynamic correlation [97, 98].

Well-known examples of a strong valence-Rydberg interaction at the CASSCF level are the excited states of ethene and butadiene [42, 82]. A similar situation was found in the anti conformer of *n*-tetrasilane (see Fig. 2), where the SA-CASSCF calculations lead to a strong mixing of the Rydberg and valence states [98]. The MS-CASPT2 method is able to rectify the problem yielding an effective separation of the computed states, which can be clearly identified as valence and Rydberg [82]. Tetrasilane can be regarded as the simplest oligosilane for which the contribution of the conformers, gauche and anti forms, on the electronic spectra can be analyzed, providing an step further to the understanding of silicon-containing compounds of great impact in modern technology [98, 99].

Table 1 compiles the results computed at the CASSCF, CASPT2, and MS-CASPT2 levels at the equilibrium geometry of the ground state using an ANO-type basis set with the contraction scheme Si[6s5p2d]/H[2s1p], which was augmented with a 1s1p1d set of Rydberg functions placed in the centre of the system. The computations were carried out within the C_{2h} symmetry constraints, with the silicon atoms placed in the *xy* plane and the *y* axis parallel to the terminal SiSi bonds. The active space comprises the σ and σ* Si–Si bond orbitals,

extended for each irreducible representation to include Rydberg orbitals and π*-symmetry Si–H antibonding orbitals, as appropriate [98].

Six valence states occur below the lowest Rydberg transition at the MS-CASPT2 level. Let us focus our attention on the singlet excited states of B_u symmetry. Transition to the lowest excited state (1^1B_u) at 6.33 eV, computed with the larger oscillator strength (around 1.12), can be clearly attributed to the low-energy experimental band with a maximum at 6.14 eV in the matrix spectrum [100]. The 1^1B_u state in terms of the occupation numbers associated with natural orbitals obtained from the PMCAS wave function corresponds to the expected one-electron promotion HOMO→LUMO of σσ* character. On the other hand, transition to the $2^1B_u(V_5)$ state at 6.96 eV has a smaller oscillator strength (0.15) and it probably contributes to the overall shape of the high-energy band with maximum at 6.89 eV observed in the matrix spectrum [99, 100]. The 3^1B_u and 4^1B_u states are 4p Rydberg states, placed at 7.46 and 7.87 eV, respectively (MS-CASPT2 results). The CASSCF calculation was carried out as four-root average of the singlet states of B_u symmetry. From a comparison of the MS-CASPT2 to the CASSCF and CASPT2 results, one can easily conclude that the CASSCF procedure leads to a too pronounced valence-Rydberg mixing that a single-reference multiconfigurational perturbation theory such as CASPT2 cannot fully recover. As a consequence, the two B_u states of valence character are placed energetically too high at the CASPT2 level, whereas the two Rydberg states are stabilized too much. Accordingly, the CASPT2 oscillator strengths for the valence transitions are underestimated (because of the interference of the Rydberg states). The opposite is true for the Rydberg transitions, which are computed with larger oscillator strengths at the CASPT2 level, with respect to the MS-CASPT2 findings, because of the mixing with the valence excited states. A comparison between the CASSCF and MS-CASPT2 results demonstrates that dynamic correlation effects contribute the most (more than 2 eV) to the excitation energy of the lowest valence excited state V_1. This effect is typically found in zwitterionic states (*i.e.,* described by hole-pair ionic VB structures) [83], which are particularly difficult to characterize theoretically.

In order to get further insight into the valence-Rydberg mixing Table 2 lists the results obtained with the Si[6s5p2d]/H[2s1p] ANO-type basis set valence basis set (omitting the Rydberg functions). The number of roots in the average CASSCF process was just the required to compute the valence excites states (2 for ^1B_u symmetry, 3 for ^1A_g symmetry including the ground state, and 1 for the remaining). As can be readily seen from Tables 1 and 2, similar results for the valence excited states are obtained with both basis sets at the MS-CASPT2 level. Furthermore, when the valence basis set is employed, the CASPT2 and MS-CASPT2 results agree (*cf.* Table 2).

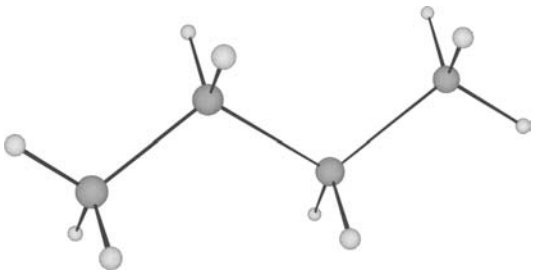

Fig. 2. The ground-state structure of the anti conformer of n-tetrasilane.

Table 1

Excitation energies (ΔE) and oscillator strengths for anti *n*-tetrasilane employing the Si[6s5p2d]/H[2s1p] + 1s1p1d (Rydberg functions) ANO-type basis set [98].

	CASSCF		CASPT2		MS-CASPT2	
State	ΔE (eV)	Osc. Str.	ΔE (eV)	Osc. Str.	ΔE (eV)	Osc. Str.
$1^1B_u(V_1)$	8.50	1.098	6.90	0.891	6.33	1.115
$2^1A_g(V_2)$	6.94	forb.	7.12	forb.	6.55	forb.
$1^1A_u(V_3)$	7.58	0.003	6.86	0.003	6.68	0.005
$3^1A_g(V_4)$	6.46	forb.	6.76	forb.	6.87	forb.
$2^1B_u(V_5)$	8.81	0.275	7.50	0.234	6.96	0.154
$1^1B_g(V_6)$	8.06	forb.	7.51	forb.	7.10	forb.
$4^1A_g(H\rightarrow 4s)$	7.10	forb.	7.33	forb.	7.40	forb.
$3^1B_u(H\rightarrow 4p)$	7.76	0.051	7.09	0.046	7.46	0.006
$2^1A_u(H\rightarrow 4p)$	7.60	0.003	7.28	0.003	7.46	0.000
$5^1A_g(H\rightarrow 3d)$	7.29	forb.	7.87	forb.	7.86	forb.
$4^1B_u(H\rightarrow 4p)$	7.79	0.279	7.13	0.255	7.87	0.029
$2^1B_g(H\rightarrow 3d)$	7.78	forb.	7.74	forb.	7.93	forb.
$6^1A_g(H\rightarrow 3d)$	7.61	forb.	7.70	forb.	7.99	forb.
$3^1B_g(H\rightarrow 3d)$	7.84	forb.	7.84	forb.	8.10	forb.
$7^1A_g(H\rightarrow 3d)$	7.76	forb.	8.09	forb.	8.22	forb.

Table 2.

Excitation energies (ΔE) and oscillator strengths for anti n-tetrasilane employing the Si[6s5p2d]/H[2s1p] ANO-type basis set [98].

	CASSCF		CASPT2		MS-CASPT2	
State	ΔE (eV)	Osc. Str.	ΔE (eV)	Osc. Str.	ΔE (eV)	Osc. Str.
$1^1B_u(V_1)$	7.98	1.542	6.40	1.237	6.36	1.175
$2^1A_g(V_2)$	7.15	forb.	6.69	forb.	6.68	forb.
$1^1A_u(V_3)$	7.39	0.003	6.66	0.002	6.66	0.002
$3^1A_g(V_4)$	7.39	forb.	6.96	forb.	6.96	forb.
$2^1B_u(V_5)$	7.84	0.121	6.88	0.107	6.92	0.165
$1^1B_g(V_6)$	7.82	forb.	7.12	forb.	7.12	forb.

However, by computing instead three roots of ^1B_u symmetry with the valence basis set, the lowest excited state moves to higher energy destroying the nice agreement with the experimental datum and the assignment for the third root is really uncertain, somewhat between valence and Rydberg character. Here we have again an unbalanced situation of valence-Rydberg mixing! Despite the one-electron basis set does not have Rydberg functions, the computation tries to simulate the 3^1B_u(H→4p) Rydberg state, as much as the diffuseness of the basis set allows. Thus, one can get good results of valence excited states using a valence basis set as long as only valence states are computed. In other words, the right number of roots for the average CASSCF step has to be considered, making sure that at the CASSCF level the valence states of a given symmetry are more stable than the Rydberg states. Unfortunately, that theoretical information comes out only from the full computation with the extended basis set. The conclusion is, therefore, that the number of valence excited states within an energy interval can only be determined from the complete consideration of both valence and Rydberg states, as it also occurs in organic compounds [15–18]. In order to achieve the goal, flexible enough basis sets have to be supplied, employing high-level methodology with inherent flexibility to overcome the possible erratic valence-Rydberg mixing. The MS-CASPT2 method in conjunction with ANO-type (valence and centred diffuse) basis set is certainly one of the low-cost possibilities. The reader can find additional discussions on the spectroscopic features of the system, as well as comparison to earlier CIS results, in the original publications [98, 99].

5.3. Computational Strategies. An Illustration: Cyclooctatetraene.

The thermal and photochemical reactivity of cyclooctatetraene (COT) has been very well studied from both experimental and theoretical standpoints (for a recent contribution see Ref. [101]). The electronic spectra of COT have comparatively received less attention, so we decided about a couple years ago to go deeply into the subject. The electron energy-loss spectrum (EELS) [102] of cycloocta-1,3,5,7-tetraene, at 50 eV impact energy and a scattering angle of 10°, can be described as a broad band of low intensity over the region 4-4.8 eV with a maximum at 4.43 eV and an intense band peaking at 6.42 eV, which has a shoulder around 6 eV. With these experimental conditions the observed features can be considered to be essentially singlet→singlet transitions [102]. The study was mainly addressed for determining the nature of those observed bands. In principle, it was expected that they could be attributed to the electronic transitions calculated vertically. The research was subsequently extended by including the singlet→triplet spectrum (relevant for the understanding of COT as triplet quencher), lowest ionization potentials, and electron affinity of COT. They shall also be briefly considered in turn. In order to design the calculation one has to decide about the equilibrium geometry of the ground state, active space, and basis set.

Previous work on the COT system clearly revealed that the ground state of neutral COT has four equivalent D_{2d} local minima connected by two independent reaction paths: ring inversion (with a D_{4h} transition state) and bond shifting (through a D_{8h} transition state) (see the 1996 landmark paper of Wenthold *et al.* [103]). Because of the tub-shaped structure belonging to the D_{2d} symmetry (see Fig. 3), both through-bond (σ-π interaction or

hyperconjugation) and through-space interactions have to be taken into account, which is a true challenge for any theoretical method [104]. On the other hand, it was also known at the time we started the project that the lowest triplet state has an octagonal structure, and that the ground state of COT radical anion is also planar belonging to the D_{4h} symmetry. A consistent treatment for the ground-state geometry optimization of these systems (neutral, lowest triplet, and radical anion) was carried out at the CASSCF level employing the π valence MOs (and the respective π electrons) active (denoted hereafter as π-CASSCF).

As illustrated in many applications, analysis of the nature and spacing of the canonical MOs is usually helpful to rationalize the most important spectroscopic features obtained from more complex CASSCF wave functions. It also serves as a qualitative guide for predicting the type of valence excited states to be computed in order to choose an active space in accordance with the expectations. This is an important step because the active space has to be supplied by the user and has, therefore, to bear enough flexibility to describe all possible type of excited states. From the electronic structure shown schematically in Fig. 4, at least five candidates can be expected as low-lying singlet excited states:

- The $^1A_2$ state described mainly by the HOMO→LUMO one-electron promotion.

- States of ^1E symmetry involving the HOMO→LUMO+1 and HOMO-1→LUMO singly excited configurations. Because of the similar orbital energy differences (12.4 eV *versus* 12.5 eV), these nearly degenerate one-electron promotions can further interact leading to a plus and minus linear combinations in the actual CASSCF wave function. As a result of the interaction, the minus and plus state are pushed down and up, respectively. The vertical transition from the ground to the minus excited state can be predicted with low intensity because of the subtraction of the corresponding transition moments. On the other hand, transition involving the plus state should carry most of the intensity. (Notice, however, that intensities are not computed but oscillator strengths).

- The $^1B_1$ state described primarily by the singly excited configuration from the deepest π orbital, $4b_2$, to the LUMO ($3a_2$).

- The $^1B_2$ state involving the highest occupied σ orbital, $3b_1$, and the LUMO.

Transitions from the ground to the $^1A_2$ and $^1B_1$ states are dipole forbidden in D_{2d} symmetry, as it is the expected transition to the $^1A_1$ state of doubly excited character. In addition, experience shows that in systems of a similar molecular size, Rydberg states converging on the lowest ionization potential are interleaved among the valence excited states. Therefore, the lowest 3s, 3p, and 3d members of the Rydberg series have also to be taken into account. The Rydberg states are described primordially by one-electron promotion from the HOMO ($5a_1$) to the 3s, 3p, 3d atomic-like MOs covering the whole molecule. The aim of the study is then clearly defined and it only remains to select the active spaces

accordingly. In this case, the process was somewhat laborious from a technical standpoint because the D_{2d} symmetry is not implemented in the software employed (MOLCAS package) [71]. Therefore, actual calculations were performing in C_{2v} symmetry. As usual, the π-valence active space was extended to include Rydberg orbitals of the different symmetries, as appropriate (see details in Ref. [105]).

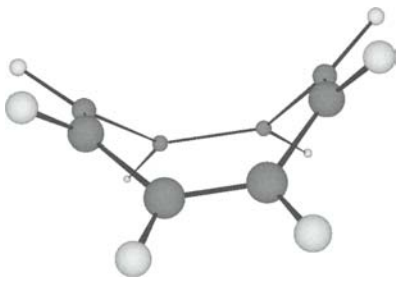

Fig. 3. The ground-state structure of cycloocta-1,3,5,7-tetraene.

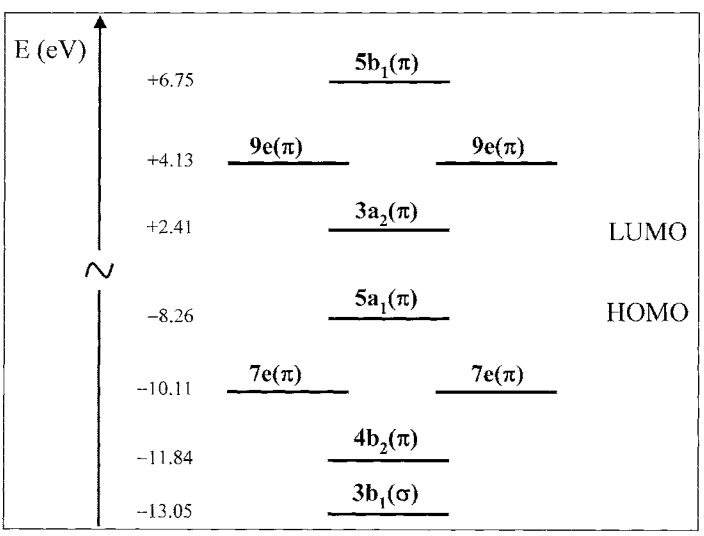

Fig. 4. Schematic electronic structure of cycloocta-1,3,5,7-tetraene including the highest five occupied and π-valence virutal canonical MOs, together with the orbital energies, computed with the ANO-type C[4s3p1d]/H[2s1p] basis set at the π-CASSCF equilibrium geometry.

The CASSCF and CASPT2 results for the vertical singlet→singlet electronic transitions obtained with the ANO-type C[4s3p1d]/H[2s1p] + 2s2p2d (Rydberg functions) basis set are listed in Table 3. The MS-CASPT2 and CASPT2 findings lead essentially to the same picture of the electronic spectrum. For the sake of simplicity only CASPT2 results shall next be considered. The computed vertical excitation energy, 3.79 eV, is somewhat too low compared to the maximum observed by electron energy-loss spectroscopy, 4.43 eV. The previous *ab initio* MRCI results reported by Palmer [106] predicted the lowest-energy band to peak at 4.37 eV. The source of the discrepancy between the MRCI results and the CASPT2 finding can be attributed to the limited basis set (split-valence quality) used for the MRCI calculations. Table 4 compiles the π-CASPT2 results computed for the lowest vertical transition $1^1A_1 \rightarrow 1^1A_2(5a_1 \rightarrow 3a_2)$ upon improving the contraction scheme. Employing the ANO-type basis set with the contraction C[3s2p]/H[2s] the CASPT2 result, 4.45 eV, is consistent with the earlier MRCI result. Thus, the message is clear. For the lowest singlet→singlet vertical transition of COT, the MRCI and CASPT2 results yield about 4.4 eV when a split-valence basis set is employed. The agreement with experiment is perfect. If we define a right theoretical result as it matches with the experimental datum, this is the typical "right answer" for the "wrong reason". Upon improving the quality of the contraction in the ANO-type basis set, which always has the same number of primitive functions, the nice agreement with the experimental datum is destroyed. Adding *d* polarization functions on the carbon atoms, the computed vertical transition drops to 3.92 eV (a similar result was obtained at the CASPT2 level with the 6-31G* basis set at a slightly different geometry) [101]. Inclusion of *p* polarization functions on the hydrogen atoms has a minor influence on the transition energy. A slight decrease of the excitation energy also occurs employing the C[4s3p1d]/H[2s1p] contraction. Adding 2s2p2d diffuse functions at the symmetry centre of the molecule, a further decrease takes place (0.11 eV with respect to the valence plus polarization basis set) and the excitation energy so computed, 3.79 eV, is similar with the result obtained with the largest valence basis set explored, 3.80 eV, which includes up to *f* and *d* functions on the carbon and hydrogen atoms, respectively. In this manner, the best theoretical estimation for the lowest vertical transition is computed to be within the energy range 3.80-4.00 eV, about half an eV below the peak observed experimentally. It seems to point out that the maximum of the low-intensity band does not correspond to the vertical excitation. Although the transition is dipole-forbidden, it is observed optically, probably through a vibronic coupling mechanism with a nearby dipole-allowed transition. If higher accuracy on theoretical grounds were required, vibronic resolution of the band would have to be performed. One of the main advantages of an *ab initio* approach relies on the fact that one is aware of the limitations introduced in the study knowing the direction to push further (if required) the methodology. It is a well-defined hierarchical framework. Pioneering INDO results [107] already predicted the $1^1A_2(5a_1 \rightarrow 3a_2)$ state around 4 eV but the deviation with respect to the experimental datum was ascribed to the inherent limitations of the semiempirical methods. On the other hand, we were curious about the performance of the TD-DFT method with the B3LYP functional to describe the electronic spectrum of COT. Employing the same geometry and the ANO-type C[4s3p1d]/H[2s1p] + 2s2p2d basis set, the lowest singlet excited state was found to be at 3.51 eV. Without the CASPT2 results at hand,

the large deviation with respect to experiment obtained by using semiempirical or TD-DFT methods could then be related to the poor performance of the methods. What are the open alternatives to solve that? Just one, to move to another parametrization and see it the result gets closer to the experimental datum. In summary, the predictive power is lost and we would have missed the main key point coming out from the *ab initio* research carried out at the CASSCF/CASPT2 level, namely the observed feature cannot be related to the vertical transition and most probably vibrational resolution of the band might be required to fully characterize it.

Table 3
Computed CASSCF and CASPT2 excitation energies (eV) and related oscillator strengths for the vertical singlet→singlet electronic transitions of cycloocta-1,3,5,7-tetraene employing the ANO-type C[4s3p1d]/H[2s1p] + 2s2p2d (Rydberg functions) basis set [105].

State	CASSCF	CASPT2	Osc. Str.	EELS data[a]
$1^1A_2(5a_1\rightarrow 3a_2)$	6.70	3.79	forbidden	4.43
$1^1E(\pi\pi^*)$	7.88	5.56	0.0075	
$2^1A_1(5a_1\rightarrow 3s)$	5.81	5.58	forbidden	
$2^1E(5a_1\rightarrow 3p_{x,y})$	6.69	5.93	0.0004	
$3^1A_1(\pi\pi^*)$	6.84	6.14	forbidden	
$1^1B_2(3b_1\rightarrow 3a_2)$	10.09	6.14	0.011	
$2^1B_2(5a_1\rightarrow 3p_z)$	6.21	6.17	0.0532	6.02
$1^1B_1(4b_2\rightarrow 3a_2)$	8.02	6.36	forbidden	
$3^1E(\pi\pi^*)$	10.28	6.40	1.1096	6.42
$5a_1\rightarrow 3d$	6.75-7.35	6.57-6.80	0.0014	

[a]Observed by electron energy-loss spectroscopy (EELS) [102].

Table 4
Convergence pattern for the lowest vertical transition $1^1A_1\rightarrow 1^1A_2(5a_1\rightarrow 3a_2)$ upon improving the contraction scheme.

Basis set[a]	π-CASPT2 (eV)	Previous (eV)
C[3s2p]/H[2s]	4.45	4.37[b]
C[3s2p1d]/H[2s]	3.92	4.00[c]
C[3s2p1d]/H[2s1p]	3.92	
C[4s3p1d]/H[2s1p]	3.90	
C[4s3p1d]/H[2s1p] + 2s2p2d	3.79[d]	
C[5s4p2d1f]/H[3s2p1d]	3.80	

[a]Primitive sets: C(14s9p4d3f)/H(8p4p3d) ANO-type basis set

[b]MRCI result [106].

[c]π-CASPT2/6-31G* result taken from Ref. [101].

[d]From Table 3.

Coming back to Table 3, the following remarks are pertinent:

- The most intense feature is related to the $3^1E(\pi\pi^*)$ state, the plus state described above. It is placed at about 10 eV at the CASSCF level and the CASPT2 result, 6.40 eV, is in agreement with experiment. The effect of dynamic correlation is crucial for the accurate location of the state. The $1^1E(\pi\pi^*)$ state corresponds to the minus state and is close to the lowest Rydberg state.

- The $3^1A_1(\pi\pi^*)$ state has a prominent weight (33.2%) of the doubly excited configuration $(HOMO\rightarrow LUMO)^2$ in the CASSCF wave function. The $3^1A_1(\pi\pi^*)$ and $1^1B_2(\sigma\pi^*)$ states are degenerate. The most plausible assignment responsible of the observed shoulder at 6.02 eV is the Rydberg transition to the $3p_z$ orbital, although the valence state $\sigma\pi^*$ might also contribute to this feature in the gas phase. The primary Rydberg character for the shoulder recorded in the gas phase is supported by the fact that it is not observed in the absorption spectrum of COT in hexane. It is well recognized that Rydberg states are usually perturbed in condensed phases and they collapse in solution. Many different earlier assignments for the observed shoulder can be found in the literature [105]. However, the issue is now clarified theoretically and it would be highly desirable that the assignment could be confirmed unambiguously by experimental research.

As we see both valence and Rydberg states coexist in the same energy region. It is more a rule than an exception for molecules of medium molecular size [15–18].

COT is employed for efficient laser operation of dye solutions because of the unique properties of its lowest triplet state. During the operation of laser dye solutions, the triplet excited levels of the dyes are populated along with the singlet states, which causes a detrimental effect in their operation. A fraction of the excited singlet state population responsible for the laser action becomes deactivated by the intersystem-crossing mechanism. These triplet dye molecules exhibit broad optical absorption triplet→triplet spectra with relatively high intensities, with the consequent loss of laser efficiency. Hence, it is essential to use a suitable triplet scavenger, able to remove the triplet dye molecules, without interfering in the laser efficiency. The acceptor COT fulfils the requirement and it is widely used for this purpose. As can be seen from Fig. 5, where the main CASPT2 results for the $S_0\rightarrow T_1$ transition are depicted, the energy difference between the vertical and adiabatic excitation energies is large, about 2 eV. Simultaneous to the electronic excitation of COT, a progressive structural reorganization towards planarity takes place. Therefore, COT has a pronounced non-vertical behavior and covers a wide range of triplet donors, $D^*(T_1)$. The origin of the $S_0\rightarrow T_1$ transition, about 0.8 eV, can be considered as an estimate of the lower limit for the triplet energy of a donor that the acceptor COT could still react with [108]. On the other hand, the vertical phosphorescence is predicted in the infrared range.

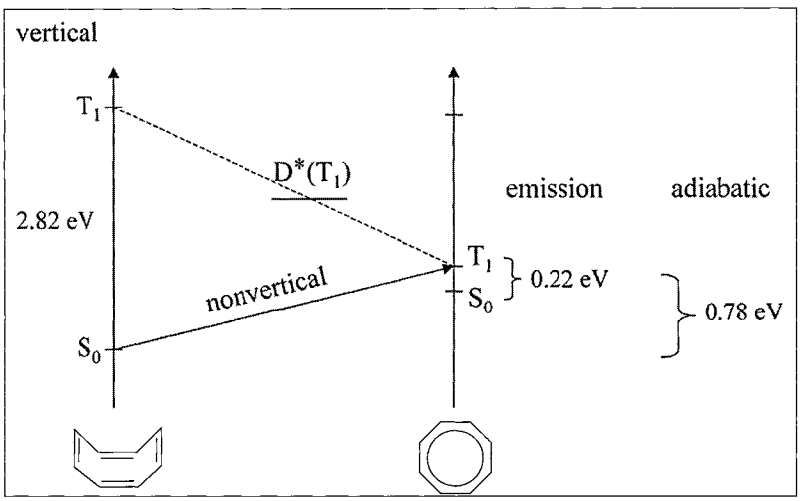

Fig. 5. The lowest singlet→triplet electronic transition. CASPT2 results for the vertical absorption, vertical emission (phosphorescence), and adiabatic excitation energies for COT. The triplet energy of a donor D is also represented.

Additional information about the lowest triplet state was obtained from the photoelectron (PE) spectrum of the radical anion, where photodetachment to two distinct electronic states of neutral COT was observed. Wenthold *et al.* [103] identified these electronic states as:

- The 1^1A_{1g} (D_{4h}) state at 1.1 eV, which corresponds to the transition state of COT ring inversion along the S_0 hypersurface, and
- The 1^3A_{2g} (D_{8h}) state; the lowest triplet state, at 1.62 eV.

Employing the ground state structure optimized for the COT radical anion, the PE spectrum was computed. At the CASPT2 level, the ground state of the neutral system is found to be at 1.11 eV and the lowest triplet state at 1.47 eV in reasonable accordance with the experimental data. As can be seen in Table 5, the results at the CASSCF level are poor. The minus sign in the CASSCF result (–0.86 eV) implies that the radical anion is not bound. Therefore, the CASPT2 approach is capable of recovering (qualitatively and quantitatively) the right relative position between the respective states of the anion and the neutral systems. It is really amazing, especially if one realizes that CASPT2 is just a second-order perturbation approach. In this type of difficult cases, involving large differential dynamic correlation contributions, the CASPT2 method certainly plays an outstanding role. Similar comments are valid for the computed electron affinity. The vertical EA is negative at both CASSCF and

CASPT2 levels of theory. Therefore, we can confidently conclude that the radical anion is not actually bound at the ground-state equilibrium geometry of COT (1^1A_1 (D_{2d})). In addition, the CASPT2 adiabatic EA, 0.56 eV, is in agreement with recent experimental determinations (0.57 eV) [109]. The agreement is entirely due to the inclusion of dynamic correlation because at the π-CASSCF level the ground-state radical anion is above the ground state of the neutral system by nearly one and half eV (−1.43 eV in Table 5).

Table 5
Computed photoelectron spectrum for the planar cyclooctatetraene radical anion and electron affinity of COT employing the ANO-type C[4s3p1d]/H[2s1p] + 2s2p2d (Rydberg functions) basis set. Energy differences in eV [105].

State	π-CASSCF	π-CASPT2	Experimental
Ground state of cyclooctatetraene radical anion: 1^2B_{1u} (D_{4h} symmetry)			
1^1A_{1g}	−0.86	1.11	1.10[a]
1^3A_{2g}	0.16	1.47	1.62[a]
vertical EA	−2.79	−0.49	
adiabatic EA	−1.43	0.56	0.57[b]

[a]Taken from the recorded photoelectron spectrum [103].

[b]See Ref. [109] and cited therein.

5.4. Up-to-date Theoretical Spectroscopy.

We shall leave for the next section the purely photochemical problems, that is, those in which different photoproducts are generated or those in which non-adiabatic state transitions occur, and focus here on spectroscopy, understood as the assignment of absorption and emission band positions and intensities, radiative lifetimes, and environmental effects. Theoretical *ab initio* spectroscopy can provide nowadays extremely accurate data that help to interpret and rationalize the experimental recordings and to predict new findings. Not all systems can be equally computed at the same level of accuracy. Excitation energies and oscillator strengths for organic systems up to the size of, for instance, the free base porphin molecule ($C_{20}N_4H_{14}$), have been studied using accurate methods and basis sets: CASPT2 [110], in which a novel interpretation of the spectrum was put forward, SAC-CI [111], and EOM-CCSD [112], although the single-configuration methods showed less accuracy. In order to compute the low-energy spectra of larger systems such as fused zinc porphyrin dimers ($Zn_2C_{40}N_8H_{22}$) at the SAC-CI level [56], severe approximations, such as lack of polarization functions in the basis sets or partial removal of virtual orbitals, were performed, undoubtedly decreasing the accuracy of the results. As a rough estimation, error boundaries smaller than 0.3 eV are required in order to obtain reliable interpretations of many spectra. DFT approaches for excited states, TD-DFT theories basically, were expected to be able to deal, although at low level of accuracy, with large systems were *ab initio* methods become too expensive. Unfortunately, recent findings have proved that the TD-DFT methods fail

dramatically in too many situations: charge transfer states [113], multiconfigurational states [113], doubly or highly-excited states [61, 113], valence states of large π extended systems such as acenes, from naphthalene to octaacene [114, 115], polyacetylene fragments or oligoporphyrins [116], polyenes, from butadiene to decapentaene [117], and the list increases every day. In some cases the errors are larger than 5 eV [114]. Regarding inorganic electronic spectroscopy, only multireference perturbation theory, CASPT2 basically, has been able to obtain general and accurate results in systems so different as ionic transition metal (TM) molecules, covalent actinide complexes or organometallic metal-ligand compounds. Typical examples are chromium hexafluoride and hexachloride anions, iron porphyrins, tetra-, penta- and hexacarbonyl or cyano TM complexes, TM dihalides, cyclometalated compounds, blue copper protein chromophores, and lanthanide and actinide oxides [16, 118–121]. The virtual extension of the multiconfigurational approaches to systems with several transition metal atoms is complicated because the selection of the reference becomes challenging [16, 118].

In the other side of the scale, *ab initio* methods can yield extremely accurate information for small systems, provided that high-level approaches and large basis sets are used. In these cases, the required accuracy is not far from the usually recognized as chemical accuracy, 1-2 kcal/mol. Not only electronic data are needed, also detailed vibrational or rotational spectroscopic information, and, typically, also vibronic or spin couplings have to be included. In very small systems, the MRCI method can be considered extremely accurate and general, provided that the problem of the size-extensivity is corrected or estimated [5, 7]. If the system fulfils certain requirements such as a closed-shell ground state well represented by a single reference and excited states of clear singly excited character, single-configuration coupled-cluster approaches including triple excitations, EOM-CCSD(T) or CC3 for instance, may offer high accuracy. Those methods are size extensive and can in practice be extended further than the MRCI approaches. In any case, the only generally applicable methods are the multireference perturbation approaches, which means, CASPT2 and related. CASPT2 is a non size-extensive methodology but, in practice, it can be shown that, in the calculation of spectroscopic properties, the corresponding effect is negligible [16]. The expected accuracy, being simply a second-order perturbation theory, cannot be as large as more elaborated approaches, except for the fact that it does not present unexpected failures in difficult cases, assuming a computation free of intruder states. As an example of the required accuracy needed to solve spectroscopic problems, a CCSD(T) study of the ground state of the van der Waals Ar-CO complex required the use of a basis set composed by aug-cc-pVQZ plus midbond functions in order to get an accuracy close to 0.3-0.4 cm^{-1} and assign conflictive rovibrational bands [122]. In general, methods for electronic excited states cannot reach the same precision.

Last decade has known tremendous breakthroughs in the field of quantum chemistry of the excited state. The number, size, and accuracy of the computed problems have grown up to the point of being comparable in certain cases with the experimental measurements, in particular for gas-phase spectroscopy. Solvent simulations in spectroscopy, basically by the Reaction Field (RF) or Quantum Mechanics/Molecular Mechanics (QM/MM) approaches, cannot be

considered quantitative so far, although they are helpful to elucidate spectroscopic assignments [2, 123, 124]. If we summarize a number of achievements made by modern quantum-chemical theories in the field of spectroscopy, it is worth remembering that, nowadays, all type of states can be computed accurately, whether valence, Rydberg or multipole-bound anionic states, optically one-photon allowed or forbidden (dark) states, and covalent, ionic, and zwitterionic states [18]. Band origins (T_e or T_0 transitions) [15–18, 42, 125] and vibrational profiles for electronic absorption and emission bands, involving ground and excited states geometry optimizations and knowledge of the states force fields are also computed with high accuracy for medium size systems such as benzene [90], pyrrole [126], and *p*-benzosemiquinone radical anion [127] leading to straightforward comparisons with experiment. Even the effects of the anharmonicities in the vibrational bands positions and intensities can be computed at different levels for, at least, small systems. As an example, the low-lying absorption and emission spectra of the formyl radical obtained at the CASPT2 level, which required the calculations of quartic potentials built by computing hundreds of points in the hypersurfaces [128]. Methods to incorporate vibronic couplings at different levels and obtain refined effects on the intensity of the vibrational bands, become also available, although at high cost [128–130]. Examples of the inclusion of accurate calculation of vibronic couplings considering the interaction of several electronic states include the CASSCF/MRCI description of the $S_2(\pi\pi^*)$ absorption band of pyrazine [130], the Green's function treatment of the photoelectron spectrum of benzene [130], and CASPT2 and EOM-CCSD studies of pyridazine and pyrimidine [131, 132]. Other consequences of the breakdown of the Born-Oppenheimer approximation such as the Jahn-Teller and Renner-Teller couplings have been widely studied in small systems, where high accuracy is needed [4]. Finally, spin-orbit couplings and relativistic effects computed at *ab initio* levels are becoming generally available for the excited states of systems including heavy atoms [4]. An example is the recent implementations of the combination of two-component relativistic formulations using a Douglas-Kroll Hamiltonian to incorporate the scalar effects and the use of multiconfigurational CASSCF/CASPT2 or shifted RASSCF methods with relativistic basis sets to solve the spin-orbit Hamiltonian. This approach proved to get errors in the relativistic effects negligible if compared with the accuracy of the methods to account for the correlation energy [133].

The whole previous discussion leads to one simple conclusion: within certain limitations related to the size of the systems, quantum-chemical methods applied to theoretical spectroscopy have reached the point where a real and constructive interplay can be established with experiment [134–137]. Both approaches, experimental and theoretical, will become more accurate in different cases. For instance, nowadays, none experimental determination can probably match the theoretical calculation of the ground-state structure for an isolated molecule, that is, modeling the system in the vapor phase. In other cases, such as hyperfine couplings at different levels or situations where the environment produce fine effects, the theoretical methods do not have enough accuracy as compared with recorded data. Apart from energies, excited states properties and transition probabilities are now routinely computed for many systems. In some cases, such as multipole moments in excited states, the

accuracy reached by the theoretical methods is also unmatched by the experimental measurements. Many representative examples can be given of this new era in the quantum chemistry of the excited state in which the *ab initio* methods, especially the multiconfigurational CASPT2 approach [15–18], have been the main protagonists. Considering the confirmed weaknesses of the TD-DFT theory to deal with excited states and the accuracy needed to solve spectroscopic problems, the *ab initio* methods will probably be the basic tool in the near future. Better implementations of the methods and development of efficient geometry optimizers will be required to proceed and they are, indeed, becoming available [84].

6. EXCITED STATES AND PHOTOCHEMISTRY

This section is devoted to the computation of excited states specifically involved in photochemical reactions, that is, reactions initiated by light. The borderline between spectroscopy and photochemistry is extremely dim and vague. We can jump from one area to the other without even notice it. For instance, if one is interested in the calculation of the vertical excitation energies of cytosine [138], the results produced are certainly in the area of theoretical spectroscopy. Now, let us assume one wants to give a step forward by computing the equilibrium structures of the main valence singlet excited states [139], namely $^1(\pi\pi^*)$, $^1(n_O\pi^*)$, and $^1(n_N\pi^*)$, one immediately enters in the field of non-adiabatic photochemistry. The CASSCF geometry optimization of the $^1(n_N\pi^*)$ state (where n_N refers to the lone pair located on the nitrogen atom) leads directly to a conical intersection with the ground state. On the other hand, the CASSCF equilibrium structure for the $^1(\pi\pi^*)$ state is essentially coincident with a conical intersection involving the excited states $^1(\pi\pi^*)$ and $^1(n_O\pi^*)$. There is no problem to reach the minimum for the $^1(n_O\pi^*)$ state, which becomes the lowest excited state at the CASSCF level [139]. However, when dynamic electron correlation is taken into account the photochemical picture is somewhat different, becoming the $^1(\pi\pi^*)$ state the most stable [140]. Incidentally, the computation of these spectroscopic properties of cytosine by employing the CIS method, with the purpose in mind of getting a rapid qualitative vision of the situation, becomes a nightmare, facing all sort of "convergence" problems (not surprisingly), leading to meaningless results where the $^1(n_O\pi^*)$ state is completely missed.

Let us start from the very beginning. Considering the excited and ground state potential energy surfaces and the different reaction paths that a system might evolve through, the molecular processes can normally be identified as photophysics, adiabatic photochemistry, and non-adiabatic photochemistry [141]. Absorption and emission can be regarded as photophysical processes. From the theoretical viewpoint they involve calculations at similar molecular structures. In an adiabatic reaction path, once that the vertical absorption takes place, the system proceeds along the hypersurface of the excited state to reach a local (or absolute) minimum leading eventually to an emitting feature. For instance, the dual fluorescence observed for dimethylaminobenzonitriles [142] and 1-phenylpyrrole [143] in polar solvents can be explained in terms of a photoadiabatic reaction that takes place in the lowest excited state. In those cases, the polar environment decreases the reaction barriers and

favors the process. In a non-adiabatic photochemical reaction path, part of the reaction occurs on the excited state hypersurface and after a non-radiative jump at the surface crossing (or funnel) continues on the ground state hypersurface. When the two hypersurfaces have the same multiplicity (*e.g.* singlet/singlet) the radiationless jump is denoted as internal conversion (IC), and intersystem crossing (ISC) is reserved for cases of different multiplicity (*e.g.* singlet/triplet). Internal conversion may occur through an avoided crossing (AC) or a conical intersection (CI). Among several researchers, Robb, Olivucci, Bernardi, and co-workers have specifically shown during the last decade the important role that conical intersections play in organic photochemistry [141]. A large number of photochemical reactivity problems has been studied in the last years involving CIs, including photoisomerizations, photocycloadditions, photorearrangements, and photodecompositions. Depending on the nature of the CI [144], the corresponding radiationless transition can yield specific photoproducts or relax the energy towards the ground-state initial situation.

Geometry determination of a conical intersection, as well as localization of minima and transition states, is usually performed at the CASSCF level. In a subsequent step, the energy differences are corrected by including dynamic correlation. If it is done at the CASPT2 level, the protocol is denoted as CASPT2//CASSCF, which stands for geometry optimization at the CASSCF level and CASPT2 calculation at the optimized CASSCF structure. Two main situations do actually occur. In cases where the PES computed at the CASSCF and CASPT2//CASSCF level behave approximately parallel (CASE A), the CASSCF optimized geometries will be in general correct, despite they have been computed at a lower level of theory. It means that dynamic correlation contributions are quite regular and similar in ample regions of the PES. The photochemistry of the protonated Schiff bases constitutes a nice CASE-A example, where the CASPT2//CASSCF computational strategy can be confidently applied. As can be seen in Fig. 3 of Ref. [145], the CASSCF minimum energy path runs parallel to that obtained at the CASPT2//CASSCF level. When dynamic correlation is markedly different for the states considered and varies significantly along the PES of interest, geometry optimization has to be carried out at the highest correlated level (CASE B). Otherwise, the uneven contributions of dynamic correlation may lead to unphysical crossings and interactions between the two electronic states. A clear representative study of CASE B corresponds to the characterization of the nature of the S_0/S_1 crossing responsible for the radiationless decay in singlet excited cytosine. The excited DNA bases have a lifetime so small that they relax to their ground state before a photochemical reaction may take place. In fact, the excited-state lifetimes of the nucleic acid molecules fall in the sub-picosecond time scale, suggesting the presence of an ultrafast internal conversion channel [146, 147]. It is an intrinsic molecular property because very short lifetimes have also been determined in the gas phase for the isolated purine and pyrimidine bases [148]. The CASPT2 results [140] suggest that the conical intersection between the ground state and the $\pi\pi^*$ state, denoted by $(gs/\pi\pi^*)_{CI}$, is responsible for the ultrafast decay of singlet excited cytosine, which is in contrast to the picture offered by the CASSCF method [139]. Moreover, the $n_O\pi^*$ state is involved in a S_2/S_1 crossing and it does not contribute directly to the ultrafast repopulation of the ground state [140]. As stated above, optimization of the singlet $n_N\pi^*$ state leads directly to

a conical intersection with the ground state but it is not found to be the preferential path of the observed decay. Whether this is a general relaxation mechanism for all the excited nucleobases or not is the subject of current research.

A situation like cytosine where the CASSCF and CASPT2 reaction paths do not run parallel (CASE B) manifests an urgent necessity of efficient algorithms for computing conical intersection with inclusion of dynamic correlation. The two main open routes available at present, through the MRCI [149] and the MS-CASPT2 methods [150], are limited to systems of small molecular size. However, in order to tackle general CASE-B problems, where the CASPT2//CASSCF (or MRCI//CASSCF) protocols are not valid, no methodology is available in practice. It is clear that most of the biomolecules of interest cannot be confidently treated today at the MRCI level because of the severe truncations that have to be performed. On the other hand, caution has to be exercised when applying the MS-CASPT2 method to locate conical intersections [151], which is next addressed by using as example the penta-2,4-dieniminium cation.

De Vico *et al.* [152] have recently reported the optimized structures for the S_1/S_0 conical intersection computed at the MS-CASPT2 and CASSCF levels, hereafter denoted as Geom. I and Geom. II, respectively. Table 6 shows the CASSCF, CASPT2, and MS-CASPT2 energy differences (ΔE) between S_1 and S_0 that we have computed at those geometries. The 6-31G* basis set was used throughout. Incidentally, because photochemical studies are mainly related to the lowest valence states, basis sets smaller than those used in spectroscopic studies, are frequently employed, which should be alright as far as no competitive Rydberg states are placed around the studied region. When the energy difference is less than 2 kcal/mol, the minimum reached is considered technically as a conical intersection; otherwise ($\Delta E \geq 2$ kcal/mol) we are facing an avoiding crossing. The MS-CASPT2(6MOs/6e) result, 3.89 kcal/mol, is similar to the CASPT2 finding employing Geom. I, and the off-diagonal matrix elements of the asymmetric effective Hamiltonian (H^{eff}) are small (less than 2 kcal/mol). Everything seems to be quite consistent. Apparently an avoiding crossing has been found at the MS-CASPT2(6MOs/6e) level. Using Geom. II, the CASSCF(6MOs/6e) and CASPT2(6MOs/6e) results for ΔE are within 1 kcal/mol. It indicates that the optimal geometry determined for the conical intersection at both levels of theory is probably very similar. However, the states become separated by 7.57 kcal/mol when they are allowed to interact. As can be seen in Table 6, the off-diagonal elements of the H^{eff} are very different, 6.12 and 1.38 kcal/mol. Because the states are nearly degenerate at the CASPT2 level, the result for the off-diagonal symmetric H^{eff} just comes out from averaging: (6.12+1.38)/2. As a consequence, the CASPT2 states are pushed down and up by that amount, 3.75 kcal/mol. Such interaction is definitely unphysical! Enlarging the active space with two extra orbitals (8MOs/6e results), which allows for radial correlation of the electrons involved in the 90°-twisted double bond, the H_{12} and H_{21} asymmetric elements become small enough, which reflects that the corresponding zeroth-order Hamiltonians are capable of yielding a balanced description for both states. Accordingly, the CASPT2 and MS-CASPT2 splitting between the S_1 and S_0 states becomes small. In summary, the computed geometry at the

CASSCF(6MOS/6e) level represents also a conical intersection at the MS-CASPT2(8MOs/6e) level, which confirms that protonated Schiff bases behave as CASE A. Unfortunately, in larger molecular systems the active space cannot be extended to the extreme that the off-diagonal elements become less than 2 kcal/mol and the MS-CASPT2 method may be forced to yield avoiding crossings. It is certainly a circumstance to be prevented in future applications of the MS-CASPT2 method.

Table 6
Energy difference between S_1 and S_0, ΔE, computed at the optimized structures of the penta-2,4-dieniminium cation S_1/S_0 conical intersection[a] at the MS-CASPT2 (Geom. I) and the CASSCF (Geom. II) levels. The 6-31G* basis set was used throughout. The off-diagonal elements of the MS-CASPT2 effective Hamiltonian (H^{eff}) are also included.

Method	Geom. I (6MOs/6e)	Geom. II (6MOs/6e)	Geom. II (8MOs/6e)
	$\Delta E(S_1-S_0)$ (kcal/mol)		
CASSCF	3.40	0.07	4.78
CASPT2	3.83	0.99	0.60
MS-CASPT2	3.89	7.57	0.64
	Off-diagonal elements of H^{eff} (kcal/mol)		
H_{12}(asymmetric)	0.62	6.12	0.18
H_{21}(asymmetric)	0.09	1.38	0.04
$H_{12}=H_{21}$ (symmetric)	0.35	3.75	0.11

[a]Optimized geometrical parameters taken from De Vico *et al.* [152].

7. FINAL REMARKS

It is clear that we are living in a new era where experimental and theoretical research can talk to each other on an equal footing. In this privileged situation we should be able to join efforts addressed to elucidate the big challenges our society faces at present in the realms of atmospheric chemistry, material science, photobiology, and nanotechnology. Experimental and theoretical research work shares at least one characteristic: the results produced have to be interpreted. The most cumbersome task is to compare experimental and theoretical derived data properly. In many cases recorded values do not directly yield the studied property, which has to be obtained by indirect procedures within a given scheme. On the other hand, theoretical results are usually obtained for simplified models. The resolution of the scientific problem certainly requires a constructive interplay between both viewpoints.

We must be able to design a research strategy in computational chemistry (RESICC) leading to results with predictive character, independent of any experimental information. Fig. 6 shows a proposed RESICC algorithm. Basic steps include:

1. Define objectives. This is surely one of the most important parts of a research. The aim of the study has to be clearly defined, as precisely as possible: What is the purpose of the computation?
2. Literature reviewing: What is the scientific background on the topic? Analysis of previous information has to be critically reviewed with open mind, because it can be extremely helpful to design the computation.
3. Actual computation. According to the previous steps the actual computation takes place at a given level of theory.
4. Once the results have been carefully analyzed two key questions rise. Are the obtained conclusions stable with respect to further theoretical improvements? Do they fulfill the initial objectives?
5. A proper action has to be taken if the calculation does not guarantee the required levels of quality. Theory has to be pushed further until stable conclusions are achieved.

It is worth noting that *ab initio* methods, because of their well-defined hierarchical structure that allows convergence of the results upon the increasing level or theory, are currently the only type of quantum-chemical tools able to fulfill the requirements implicit in the RESICC scheme. The decision is up to you!

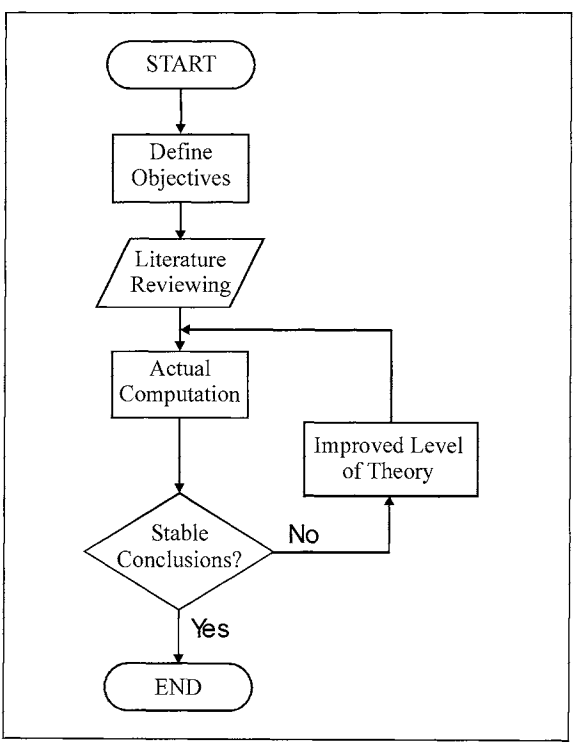

Fig. 6. Research strategy in computational chemistry.

8. ACKNOWLEDGMENTS

We thank our co-workers for their valuable contributions. MCYT of Spain, projects BQU2001-2926 and BQU2004-01739, and *Generalitat Valenciana*, project GV04B-228, have financed the research.

REFERENCES

[1] A. Szabo and N.S. Ostlund, Modern Quantum Chemistry, McGraw-Hill, New York, 1989.

[2] C.J. Cramer, Essentials of Computational Chemistry, Wiley, Chichester, 2002.

[3] T. Veszprémi and M. Fehér, Quantum Chemistry. Fundamentals to Applications, Kluwer, Dordretch, 1999.

[4] P. Jensen and P.R. Bunker (eds.), Computational Molecular Spectroscopy, Wiley, Chichester, 2000.

[5] B.O. Roos and P.E.M. Siegbahn, Int. J. Quantum Chem., 17 (1980) 485-500.

[6] S. Peyerimhoff, Spectroscopy: Computational Methods, in Encyclopedia of Computational Chemistry, P.v.R. Schleyer *et al.* (eds.), Wiley, Chichester, 1998, pp. 2646-2664.

[7] R.J. Buenker, G. Hirsch, Y. Li, J.-P. Gu, A.B. Alekseyev, H.-P. Liebermann, and M. Kimura, *Ab Initio* Calculations of Excited State Potential Functions, in Computational Molecular Spectroscopy, P. Jensen and P. R. Bunker (eds.), Wiley, Chichester, 2000, pp. 135-168.

[8] J.L. Heully, J.P. Malrieu, I. Nebot-Gil, and J. Sánchez-Marín, Chem. Phys. Lett., 256 (1996) 589-594.

[9] E.R. Davidson and L.E. McMurchie, *Ab Initio* Calculations of Excited-State Potential Surfaces of Polyatomic Molecules, in Excited States, E.C. Lim (ed.), Academic Press, London, 1982, pp. 1-35.

[10] K. Andersson, P.–Å. Malmqvist, and B.O. Roos, J. Chem. Phys., 96 (1992) 1218-1226.

[11] K. Andersson and B.O. Roos, Chem. Phys. Lett., 191 (1992) 507-514.

[12] B.O. Roos, K. Andersson, and M.P. Fülscher, Chem. Phys. Lett., 192 (1992) 5-13.

[13] K. Hirao (ed.), Recent Advances in Multireference Methods, World Scientific Publishing, Singapore, 1999.

[14] P. Knowles, M. Schütz, and H.-J. Werner, in Modern Methods and Algorithms of Quantum Chemistry, J. Grotendorst (ed.), John von Neumann Institute for Computing, NIC Series, Vol 1, Jülich, 2000, pp. 69-151.

[15] B.O. Roos, M.P. Fülscher, P.-Å. Malmqvist, M. Merchán, and L. Serrano-Andrés, in Quantum Mechanical Electronic Structure Calculations with Chemical Accuracy, S. R. Langhoff (ed.), Kluwer Academic Publishers, Dordrecht, 1995, pp. 357-438.

[16] B.O. Roos, M.P. Fülscher, P.-Å. Malmqvist, L. Serrano-Andrés, K. Pierloot, and M. Merchán, in Advances in Chemical Physics: New Methods in Computational Quantum Mechanics, I. Prigogine and S. A. Rice (eds.), John Wiley and Sons, New York, 1996, pp- 219-331.

[17] M. Merchán, L. Serrano-Andrés, M.P. Fülscher, and B.O. Roos, in Recent Advances in Multireference Methods, K. Hirao (ed.), World Scientific Publishing, Singapore, 1999.

[18] L. Serrano-Andrés and M. Merchán, in Encyclopedia of Computational Chemistry, P.v.R. Schleyer *et al.* (eds.), Wiley, Chichester, 2004.

[19] J.B. Foresman, M. Head-Gordon, J.A. Pople, and M.J. Frisch, J. Phys. Chem., 96 (1992) 135-149.

[20] J. Oddershede, Propagator Methods, in *Ab Initio* Methods in Quantum Chemistry II, Advances in Chemical Physics, Vol. 69, K. P. Lawley (ed.), Wiley, Chichester, 1987, pp. 201-239.

[21] H. Nakatsuji, Chem. Phys. Lett., 67 (1979) 334-342.

[22] J.F. Stanton and R.J. Bartlett, J. Chem. Phys., 98 (1993) 7029-7039.

[23] O. Christiansen, H. Koch, and P. Jørgensen, Chem. Phys. Lett., 243 (1995) 409-418.

[24] F. Illas, M. Merchán, M. Pélissier, and J.P. Malrieu, Chem. Phys., 107 (1986) 361-380.

[25] P.O. Löwdin, Annu. Rev. Phys. Chem., 11 (1960) 107-132.

[26] C.C.J. Roothaan, Rev. Mod. Phys., 23 (1951) 69-89.

[27] A.C. Hurley, Introduction to the Electron Theory of Small Molecules, Academic Press, New York, 1976.

[28] B.O. Roos, in Multiconfigurational (MC) Self-Consistent (SCF) Theory: European Summerschool in Quantum Chemistry, Vol. 2, B.O. Roos and P.-O. Widmark (eds.), Lund University, 2000, pp. 285-359.

[29] R. González-Luque, M. Merchán, and B.O. Roos, Theor. Chim. Acta, 88 (1994) 425-435.

[30] R. J. Gdanitz and R. Ahlrichs, Chem. Phys. Lett., 143 (1988) 413-420.

[31] P.-Å. Malmqvist, A. Rendell, and B.O. Roos, J. Phys. Chem., 94 (1990) 5477-5482.

[32] R. González-Luque, M. Merchán, M.P. Fülscher, and B.O. Roos, Chem. Phys. Lett., 204 (1993) 323-332.

[33] H. Partridge, S.R. Langhoff, C.W. Bauschlicher Jr, in Quantum Mechanical Electronic Structure Calculations with Chemical Accuracy, S.R. Langhoff (ed.), Kluwer Academic Publishers, Dordrecht, 1995, pp. 209-260.

[34] M. Cantos, M. Merchán, F. Tomás-Vert, and B.O. Roos, Chem. Phys. Lett., 229 (1994) 181-190.

[35] T. Helgaker, P. Jørgensen, and J. Olsen, Molecular Electronic-Structure Theory, Wiley, Chichester, 2000.

[36] M. Head-Gordon, R.J. Rico, M. Oumi, and T.J. Lee, Chem. Phys. Lett., 219 (1994) 21-29.

[37] R.E. Stratmann, G.E. Scuseria, and M.J. Frisch, J. Chem. Phys., 109 (1998) 8218-8224.

[38] V. Molina, B.R. Smith, and M. Merchán, Chem. Phys. Lett., 309 (1999) 486–494.

[39] L. Serrano-Andrés, M. Merchán, and M. Jablonski, J. Chem. Phys., 119 (2003) 4294-4304.

[40] A.C. Borin, L. Serrano-Andrés, V. Ludwig, and S. Canuto, Phys. Chem. Chem. Phys., 5 (2003) 5001-5009.

[41] K.B. Wiberg, C.M. Hadad, G.B. Ellison, and J.B. Foresman, J. Phys. Chem., 97 (1993) 13586-13597.

[42] L. Serrano-Andrés, M. Merchán, I. Nebot-Gil, R. Lindh, and B.O. Roos, J. Chem. Phys., 98 (1993) 3151-3162.

[43] J. Lappe and R.J. Cave, J. Phys. Chem., 104 (2000) 2294-2300.

[44] M. Merchán, L. Serrano-Andrés, L.S. Slater, B.O. Roos, R. McDiarmid, and X. Xing, J. Phys. Chem. A, 103 (1999) 5468-5476.

[45] J. Olsen and P. Jørgensen, J. Chem. Phys., 82 (1985) 3235-3264.

[46] P. Jørgensen and J. Simons, Second Quantization-Based Methods in Quantum Chemistry, Academic Press, New York, 1981.
[47] E.S. Nielsen, P. Jørgensen, and J. Oddershede, J. Chem. Phys., 73 (1980) 6238-6246.
[48] M.J. Packer, E.K. Dalskov, T. Enevoldsen, H.J. Aa. Jensen, and J. Oddershede, J. Chem. Phys., 105 (1996) 5886-5900.
[49] A.B. Trofimov, G. Stelter, and J. Schirmer, J. Chem. Phys., 117 (2002) 6402-6410.
[50] O. Christiansen, K.L. Bak, H. Koch, and S.P.A. Bauer, Chem. Phys. Lett., 284 (1998) 47-55.
[51] P. Cronstrand, O. Christiansen, P. Norman, and H. Ågren, Phys. Chem. Chem. Phys., 2 (2000) 5357-5363.
[52] J.W. Krogh and J. Olsen, Chem. Phys. Lett., 344 (2001) 578-586.
[53] M. Tobita, S.S. Perera, M. Musial, R.J. Bartlett, M. Nooijen, and J.S. Lee, J. Chem. Phys., 119 (2003) 10713-10723.
[54] K. Kowalski and P. Piecuch, J. Chem. Phys., 120 (2004) 1715-1738.
[55] T.J. Lee and G.E. Scuseria, in Quantum Mechanical Electronic Structure Calculations with Chemical Accuracy, S.R. Langhoff (ed.), Kluwer Academic Publishers, Dordrecht, 1995, pp. 47-108.
[56] T. Miyahara, H. Nakatsuji, J. Hasegawa, A. Osuka, N. Aratani, and A. Tsuda, J. Chem. Phys., 117 (2002) 11196-11207.
[57] K. Hirao, J. Chem. Phys., 95 (1991) 3589-3595.
[58] M. Musial, S.A. Kucharski, and R.J. Bartlett, J. Chem. Phys., 118 (2003) 1128-1136.
[59] H. Koch and P. Jørgensen, J. Chem. Phys., 93 (1990) 3333-3344.
[60] H. Koch, O. Christiansen, P. Jørgensen, and J. Olsen, Chem. Phys. Lett., 244 (1995) 75-82.
[61] M. Parac and S. Grimme, J. Phys. Chem. A, 106 (2002) 6844-6850.
[62] J.D. Watts and R.J. Bartlett, Chem. Phys. Lett., 258 (1996) 581-588.
[63] K.W. Sattelmeyer, J.F. Stanton, J. Olsen, and J. Gauss, Chem. Phys. Lett., 347 (2001) 499-504.
[64] S. Chattopadhyay, U.S. Mahapatra, and D. Mukherjee, in Recent Advances in Multireference Methods, K. Hirao (ed.), World Scientific Publishing, Singapore, 1999.
[65] S.P.A. Sauer and M.J. Packer, The *Ab Initio* Calculation of Molecular Properties Other than the Potential Energy Surface, in Computational Molecular Spectroscopy, P. Jensen and P.R. Bunker (eds.), Wiley, Chichester, 2000, pp. 221-252.
[66] S. Grimme and M. Waletzke, J. Chem. Phys., 111 (1999) 5645-5655.
[67] T. Nakajima and H. Nakatsuji, Chem. Phys. Lett., 280 (1997) 79-84.
[68] J.F. Stanton and J. Gauss, J. Chem. Phys., 100 (1994), 4695-4698.
[69] A. Kohn and C. Hattig, J. Chem. Phys., 119 (2003) 5021-5036.
[70] K. P. Lawley (ed.), *Ab Initio* Methods in Quantum Chemistry, Part II, Wiley, Chichester, 1987.
[71] K. Andersson, M. Baryz, A. Bernhardsson, M.R.A. Blomberg, P. Boussard, D.L. Cooper, T. Fleig, M.P. Fülscher, B. Hess, G. Karlström, R. Lindh, P.–Å. Malmqvist, P. Neogrády, J. Olsen, B.O. Roos, A.J. Sadlej, B. Schimmelpfennig, M. Schütz, L. Seijo, L. Serrano-Andrés, P.E.M. Siegbahn, J. Stålring, T. Thorsteinsson, V. Veryazov, U. Wahlgren, P.-O. Widmark, *MOLCAS, version 5.0*; Department of Theoretical Chemistry, Chemical Centre, University of Lund, P.O.B. 124, S-221 00 Lund: Sweden, 2000.
[72] B.O. Roos and P.R. Taylor, Chem. Phys., 48 (1980) 157-173.
[73] A.D. McLean and B. Liu, J. Chem. Phys., 58 (1973) 1066-1078.

[74] B.O. Roos, K. Andersson, M.P. Fülscher, L. Serrano-Andrés, K. Pierloot, M. Merchán, and V. Molina, J. Mol. Struct. (Theochem), 388 (1996) 257-276.
[75] K. Hirao, Chem. Phys. Lett., 190 (1992) 374-380.
[76] P.M. Kozlowski and E.R. Davidson, J. Chem. Phys., 100 (1994) 3672-3682.
[77] J.P. Finley and K.F. Freed, J. Chem. Phys., 102 (1995) 1306-1333.
[78] A. Zaitsevskii and J.P. Malrieu, Chem. Phys. Lett., 233 (1995) 597-604.
[79] H. J. Werner, Mol. Phys., 89 (1996) 645-661.
[80] S. Grimme and M. Waletzke, Phys. Chem. Chem. Phys., 2 (2000) 2075-2081.
[81] B.O. Roos, A Perturbation-Variation Treatment of the Multi-State Problem in CASPT2, Lund University, 1996.
[82] J. Finley, P.-Å. Malmqvist, B.O. Roos, and L. Serrano-Andrés, Chem. Phys. Lett., 288 (1998) 299-306.
[83] M. Klessinger and J. Michl, Excited States and Photochemistry of Organic Molecules, VCH Publishers, New York, 1995.
[84] P. Celani and H.-J. Werner, J. Chem. Phys., 119 (2003) 5044-5047.
[85] M.P. Dallos, T. Müller, H. Lischka, and R. Shepard, J. Chem. Phys., 114 (2001) 746-757.
[86] S.S. Han and D.S. Yarkony, J. Chem. Phys., 119 (2003) 11561-11569.
[87] A.J.C. Varandas, On the Geometric Phase Effect in Jahn-Teller Systems, in Fundamental World of Quantum Chemistry, Vol II, E.J. Brändas and E.S. Kryachko (eds.), Kluwer, Netherlands, 2003, pp. 33-92.
[88] P.R. Taylor, in Accurate Calculations and Calibration: European Summerschool in Quantum Chemistry, Vol. 3, B.O. Roos and P.-O. Widmark (eds.), Lund University, 2000, pp. 667-676.
[89] T. Müller, M. Dallos, and H. Lischka, J. Chem. Phys., 110 (1999) 7176-7184.
[90] A. Bernhardsson, N. Forsberg, P.-Å. Malmqvist, B.O. Roos, and L. Serrano-Andrés, J. Chem. Phys., 112 (2000) 2798-2809.
[91] C. Page, M. Merchán, L. Serrano-Andrés, and M. Olivucci, J. Phys. Chem. A, 103 (1999) 9864-9871.
[92] L. Serrano-Andrés, R. Lindh, B.O. Roos, and M. Merchán, J. Phys. Chem., 97 (1993) 9360-9368.
[93] V. Molina, M. Merchán, and B.O. Roos, J. Phys. Chem. A, 101 (1997) 3478-3487.
[94] J.R. Lakowicz, Principles of Fluorescence Spectroscopy, Kluwer, New York, 1999.
[95] J.L. McHale, Molecular Spectroscopy, Prentice Hall, Upper Saddle River, 1999.
[96] N.J. Turro, Modern Molecular Photochemistry, University Science Books, Sausalito, 1991.
[97] M. Merchán, R. González-Luque, and B.O. Roos, Theor. Chim. Acta, 94 (1996) 143-154.
[98] R. Crespo, M. Merchán, and J. Michl, J. Phys. Chem. A, 104 (2000) 8593-8599.
[99] M.C. Piqueras, M. Merchán, R. Crespo, and J. Michl, J. Phys. Chem. A, 106 (2002) 9868-9873.
[100] B. Albinsson, H. Teramae, H.S. Plitt, L.M. Goss, H. Schmidbaur, and J. Michl, J. Phys. Chem., 100 (1996) 8681-8691.
[101] M. Garavelli, F. Bernardi, A. Cembran, O. Castaño, L.M. Frutos, M. Merchán, and M. Olivucci, J. Am. Chem. Soc., 124 (2002) 13770-13789.
[102] R.P. Frueholz and A. Kuppermann, J. Chem. Phys., 69 (1978) 3614-3621.
[103] P.G. Wenthold, D.P. Hrovath, W.T. Borden, and W.C. Lineberger, Science, 272 (1996) 1456-1459.

[104] B.O. Roos, M. Merchán, R. McDiarmid, and X. Xing, J. Am. Chem. Soc., 116 (1994) 5927-5936.
[105] L.-M. Frutos, O. Castaño, and M. Merchán, J. Phys. Chem. A, 107 (2003) 5472-5478.
[106] M.H. Palmer, J. Mol. Struct., 178 (1988) 79-87.
[107] F.A. Van-Catledge, J. Am. Chem. Soc., 93 (1971) 4365-4374.
[108] L.M. Frutos, O. Castaño, J.L. Andrés, M. Merchán, and A.U. Acuña, J. Chem. Phys., 120 (2004) 1208-1216.
[109] T.M. Miller, A.A. Viggiano, and A.E.S. Miller, J. Phys. Chem. A, 106 (2002) 10200-10204.
[110] L. Serrano-Andrés, M. Merchán, M. Rubio, and B.O. Roos, Chem. Phys. Lett., 295 (1998) 195-203.
[111] H. Nakatsuji, J.Y. Hasegawa, and M. Hada, J. Chem. Phys., 104 (1996) 2321-2329.
[112] M. Nooijen and R.J. Bartlett, J. Chem. Phys., 106 (1997) 6449-6455.
[113] D.J. Tozer, R.D. Amos, N.C. Handy, B.O. Roos, and L. Serrano-Andrés, Mol. Phys., 97 (1999) 859-868.
[114] M. Parac and S. Grimme, Chem. Phys. 292 (2003) 11-21.
[115] S. Grimme and M. Parac, ChemPhysChem, 3 (2003) 292-295.
[116] Z.-L. Cai, K. Sendt, and J.R. Reimers, J. Chem. Phys., 117 (2002) 5543-5549.
[117] M. Wanko, M. Garavelli, F. Bernardi, T.A. Niehaus, T. Frauenheim, and M. Elstner, J. Chem. Phys., 120 (2004) 1674-1692.
[118] K. Pierloot, Mol. Phys., 13 (2003) 2083-2094.
[119] K. Pierloot, A. Ceulemans, M. Merchán, and L. Serrano-Andrés, J. Phys. Chem. A, 104 (2000) 4374-4382.
[120] U. Ryde, M.H.M. Olsson, B.O. Roos, K. Pierloot, J.O.A. De Kerpel, Protein, Blue Copper: Electronic Spectra, in Encyclopedia of Computational Chemistry, P. v. R. Schleyer *et al.* (eds.), Wiley, Chichester, 1998, pp. 2255-2270.
[121] B.O. Roos, P.-O. Widmark, and L. Gagliardi, Faraday Discuss., 124 (2003) 57-62.
[122] J. López-Cacheiro, B. Fernández, T.B. Pedersen, and H. Koch, J. Chem. Phys., 118 (2003) 9596-9607.
[123] L. Serrano-Andrés, M.P. Fülscher, and G. Karlström, Int. J. Quantum Chem., 65 (1997) 167-181.
[124] N. Ferré and M. Olivucci, J. Am. Chem. Soc., 125 (2003) 6868-6869.
[125] L. Serrano-Andrés and B.O. Roos, J. Am. Chem. Soc., 118 (1996) 185-195.
[126] B. O. Roos, P.-Å. Malmqvist, V. Molina, L. Serrano-Andrés, and M. Merchán, J. Chem. Phys., 116 (2002) 7526-7537.
[127] R. Pou-Amérigo, L. Serrano-Andrés, M. Merchán, E. Ortí, and N. Forsberg, J. Am. Chem. Soc., 122 (2000) 6067-6077.
[128] L. Serrano-Andrés, N. Forsberg, and P.-Å. Malmqvist, J. Chem. Phys., 108 (1998) 7202-7216.
[129] G. Fischer, Vibronic Coupling, Academic Press, London, 1984.
[130] H. Köppel and W. Domcke, Vibronic Dynamics in Polyatomic Molecules, in Encyclopedia of Computational Chemistry, P.v.R. Schleyer *et al.* (eds.), Wiley, Chichester, 1998, pp. 3166-3182.
[131] G. Fischer and P. Wormell, Chem. Phys., 257 (2000) 1-20.
[132] G. Fischer, Z.L. Cai, J.R. Reimers, and P. Wormell, J. Phys. Chem. A, 107 (2003) 3093-3106.
[133] P.-Å. Malmqvist, B.O. Roos, and B. Schimmelpfennig, Chem. Phys. Lett., 357 (2002) 230-240.

[134] M. Merchán, B.O. Roos, R. McDiarmid, and X. Xing, J. Chem. Phys., 104 (1996) 1791-1804.
[135] J.P. Dinnocenzo, M. Merchán, B.O. Roos, S. Shaik, and H. Zuilhof, J. Phys. Chem. A, 102 (1998) 8979-8987.
[136] L. Serrano-Andrés and M.P. Fülscher, J. Phys. Chem. B, 105 (2001) 9323-9330.
[137] V. Molina and M. Merchán, Proc. Nat. Acad. Sci. USA, 98 (2001) 4299-4304.
[138] M.P. Fülscher and B.O. Roos, J. Am. Chem. Soc., 117 (1995) 2089-2095.
[139] N. Ismail, L. Blancafort, M. Olivucci, B. Kohler, and M.A. Robb, J. Am. Chem. Soc., 124 (2002) 6818-6819.
[140] M. Merchán and L. Serrano-Andrés, J. Am. Chem. Soc., 125 (2003) 8108-8109.
[141] M. A. Robb, M. Olivucci, and F. Bernardi, Photochemistry, in Encyclopedia of Computational Chemistry, P.v.R. Schleyer *et al.* (eds.), Wiley, Chichester, 1998, pp. 2056-2064.
[142] L. Serrano-Andrés, M. Merchán, R. Lindh, and B.O. Roos, J. Am. Chem. Soc., 117 (1995) 3189-3202.
[143] B. Proppe, M. Merchán, and L. Serrano-Andrés, J. Phys. Chem. A, 104 (2000) 1608-1616.
[144] G.J. Atchity, S.S. Xantheas, and K. Ruedenberg, J. Chem. Phys., 95 (1991) 1862-1876.
[145] R. González-Luque, M. Garavelli, F. Bernardi, M. Merchán, M.A. Robb, and M. Olivucci, Proc. Nat. Acad. Sci. USA, 97 (2000) 9379-9384.
[146] J.-M. Pecourt, J. Peon, and B. Kohler, J. Am. Chem. Soc., 123 (2001) 10370-10378.
[147] J. Peon and A.H. Zewail, Chem. Phys. Lett., 348 (2001) 255-262.
[148] H. Kang, K.T. Lee, B. Jung, Y.J. Ko, and S.K. Kim, J. Am. Chem. Soc., 124 (2002) 12958-12959.
[149] D.R. Yarkony, J. Phys. Chem. A, 105 (2001) 6277-6293.
[150] C.S. Page and M. Olivucci, J. Comput. Chem., 24 (2003) 298-309.
[151] L. Serrano-Andrés, M. Merchán, and R. Lindh, to be published.
[152] L. De Vico, C.S. Page, M. Garavelli, F. Bernardi, R. Basosi, and M. Olivucci, J. Am. Chem. Soc., 124 (2002) 4124-4134.